frontiers in Marine Science

ORIGINAL RESEARCH
published: 05 November 2021
doi: 10.3389/fmars.2021.750658

Viral-Like Particles Are Associated With Endosymbiont Pathology in Florida Corals Affected by Stony Coral Tissue Loss Disease

Thierry M. Work[1], Tina M. Weatherby[2], Jan H. Landsberg[3], Yasunari Kiryu[3], Samantha M. Cook[4] and Esther C. Peters[4]*

[1] National Wildlife Health Center, Honolulu Field Station, United States Geological Survey, Honolulu, HI, United States, [2] Biological Electron Microscope Facility, Pacific Biosciences Research Center, University of Hawai'i at Mānoa, Honolulu, HI, United States, [3] Fish and Wildlife Research Institute, Florida Fish and Wildlife Conservation Commission, St. Petersburg, FL, United States, [4] Department of Environmental Science and Policy, George Mason University, Fairfax, VA, United States

OPEN ACCESS

Edited by:
William F. Precht, Dial Cordy and Associates, Inc., United States

Reviewed by:
Mark E. Warner, University of Delaware, United States
Karen Lynn Neely, Nova Southeastern University, United States
Adrienne M. S. Correa, Rice University, United States

***Correspondence:**
Thierry M. Work
Thierry_Work@usgs.gov

Specialty section:
This article was submitted to Coral Reef Research, a section of the journal Frontiers in Marine Science

Received: *30 July 2021*
Accepted: *18 October 2021*
Published: *05 November 2021*

Citation:
Work TM, Weatherby TM, Landsberg JH, Kiryu Y, Cook SM and Peters EC (2021) Viral-Like Particles Are Associated With Endosymbiont Pathology in Florida Corals Affected by Stony Coral Tissue Loss Disease. Front. Mar. Sci. 8:750658. doi: 10.3389/fmars.2021.750658

Stony coral tissue loss disease (SCTLD) was first documented in 2014 near the Port of Miami, Florida, and has since spread north and south along Florida's Coral Reef, killing large numbers of more than 20 species of coral and leading to the functional extinction of at least one species, *Dendrogyra cylindrus*. SCTLD is assumed to be caused by bacteria based on presence of different molecular assemblages of bacteria in lesioned compared to apparently healthy tissues, its apparent spread among colonies, and cessation of spread of lesions in individual colonies treated with antibiotics. However, light microscopic examination of tissues of corals affected with SCTLD has not shown bacteria associated with tissue death. Rather, microscopy shows dead and dying coral cells and symbiotic dinoflagellates (endosymbionts) indicating a breakdown of host cell and endosymbiont symbiosis. It is unclear whether host cells die first leading to death of endosymbionts or vice versa. Based on microscopy, hypotheses as to possible causes of SCTLD include infectious agents not visible at the light microscopy level or toxicosis, perhaps originating from endosymbionts. To clarify this, we examined corals affected with SCTLD and apparently healthy corals using transmission electron microscopy. Endosymbionts in SCTLD-affected and apparently healthy corals consistently had varying degrees of pathology associated with elongated particles compatible in morphology with filamentous positive single-stranded RNA viruses of plants termed anisometric viral-like particles (AVLP). There was apparent progression from early to late replication of AVLP in the cytoplasm of endosymbionts adjacent to or at times within chloroplasts, with morphologic changes in chloroplasts consistent with those seen in plant cells infected by viruses. Coral host cell pathology appeared limited to massive proliferation and lysis of mucus cells. Based on these findings, we hypothesize that SCTLD is a viral disease of endosymbionts leading to coral host death. Efforts to confirm the presence of a virus associated with SCTLD

through other means would be appropriate. These include showing the presence of a virus through molecular assays such as deep sequencing, attempts to grow this virus in the laboratory through culture of endosymbionts, localization of virus in tissue sections using immunohistochemistry or *in situ* hybridization, and experimental infection of known-virus-negative corals to replicate disease at the gross and microscopic level.

Keywords: stony coral tissue loss disease, Symbiodiniaceae, zooxanthellae, transmission electron microscopy, Flexiviridae, pathogenesis

INTRODUCTION

Stony coral tissue loss disease (SCTLD) was first identified in 2014 near Virginia Key off Miami, Florida (Precht et al., 2016; Aeby et al., 2019), and has spread to the northernmost extent of Florida's Coral Reef (FCR), south through the Florida Keys and multiple distant sites. The disease is severe enough to have led to functional extinction of at least one species of coral, *Dendrogyra cylindrus* in Florida (Neely et al., 2021). SCTLD presents as varying degrees of acute to subacute tissue loss, variably bordered by focal bleaching, affecting more than 20 species of corals (Florida Coral Disease Response Research and Epidemiology Team, 2018; Aeby et al., 2019) and is assumed by some to be caused by an infectious agent (Muller et al., 2020). Supporting this hypothesis is a spatial epidemiology suggestive of a contagion (Muller et al., 2020), corals affected by SCTLD have specific groups of bacteria associated with lesions as detected by molecular assays (Meyer et al., 2019; Rosales et al., 2020; Ushijima et al., 2020), and multiple species of affected corals respond positively to treatments with antibiotics (Neely et al., 2020, 2021), although this practice does not prevent genesis of additional lesions (Shilling et al., 2021; Walker et al., 2021). Finally, experimental mesocosm studies suggest SCTLD is transmissible (Aeby et al., 2019; Eaton et al., 2021; Meiling et al., 2021).

Contradicting the possibility that bacteria cause SCTLD are light microscopy descriptions of the disease that have, to date, not shown bacteria or any other organism associated with cell pathology such as visible evidence of bacterial clusters adjacent to dead cells (Landsberg et al., 2020). Instead, endosymbiotic dinoflagellate algae from the family Symbiodiniaceae (endosymbionts) living in the gastrodermal cells of the corals' polyps (LaJeunesse et al., 2018) and coenenchyme were degenerating at, as well as some distance away from, the tissue-loss margins, suggesting that they were more sensitive to damaging factors than the corals' cells. Thus, histopathology indicates that SCTLD appears to be a dysfunction of the symbiotic relationship between host and endosymbionts leading to death of endosymbionts and host cells and gross clinical signs of tissue loss and focal bleaching (Landsberg et al., 2020). Based on microscopic findings, the hypothesis is that either endosymbionts are dying leading to host cell death or vice versa. Because light microscopy cannot, in general, resolve microorganisms smaller than bacteria, SCTLD could be caused by smaller infectious agents such as viruses. Alternatively, SCTLD could be some sort of toxicosis that leads to host cell lysis (Landsberg et al., 2020). Dinoflagellates are known to produce a variety of toxic substances that can be harmful to humans and aquatic animals (Landsberg, 2002), so plausibly, endosymbionts might be producing toxins that kill the coral host. Indeed, studies exist documenting production of toxins in endosymbiotic dinoflagellates from corals (Nakamura et al., 1993) some of which are implicated in pathogenesis of coral bleaching (McConnaughey, 2012).

The role of viruses in causing cell pathology in corals is not well explored. Most work on coral viruses has focused on molecular deep sequencing studies to assess presence of viruses in coral reef environments, a topic reviewed extensively (Vega Thurber and Correa, 2011; Vega-Thurber et al., 2017). According to these authors, viruses infect coral cells, symbionts, and bacteria associated with corals. Based on molecular presence of viruses in various geographic locations or associations of these with various disease states, certain viruses, like bacteriophages, play a potential role in nutrient cycling by lysing bacteria. Bacteriophages are also thought to be protective against certain bacterially induced diseases in corals. Finally, shifts in viromes associated with bleaching in corals also implicate a potential role of viruses in coral health. For instance, a bleaching event in *Acropora* from the Pacific revealed molecular and transmission electron microscopy (TEM) evidence of a herpesvirus association (Correa et al., 2016). Experimental studies have also tried to induce virus replication in cultured symbionts from a variety of corals from the Pacific and visualizing these endosymbionts with TEM. Examples include detection of viral-like particles in endosymbionts of *Euphyllia paradivisa* exposed to particulate organic matter (Rosset et al., 2015), *Acropora digitifera*, *Echinopora hirsutissima*, *Porites rus*, *Pocillopora damicornis*, and *P. damicornis* exposed to UV and far-red radiation (Camaya et al., 2016). In all those cases, the viruses had icosahedral morphology. In contrast, filamentous viral-like particles were also seen in TEM studies of UV or heat-stressed endosymbionts from unspecified Cnidaria by Lohr et al. (2007), and studies with *Acropora tenuis* by Weynberg et al. (2017). Less effort has been expended on looking at viruses in Caribbean corals. One instance is the discovery of single-stranded RNA viruses in *Montastraea cavernosa* (Correa et al., 2013), but their role in disease causation was unclear.

Transmission electron microscopy allows for detection of very small structures like cell organelles and viruses. The purpose of this study was to examine tissues from SCTLD-affected and apparently healthy corals by using TEM to characterize the disease at the ultrastructural level in attempts to relate light microscopic findings to those from TEM, clarify whether endosymbionts or host cells die first, and see if infectious agents could be associated with cell pathology.

MATERIALS AND METHODS

Samples were collected from coral colonies from various locations in Florida during 2016 and 2018 by Florida's Fish and Wildlife Conservation Commission (FWC) Fish and Wildlife Research Institute (FWRI) and preserved in TEM (Trump's) fixative (McDowell and Trump, 1976) as described in Landsberg et al. (2020). Briefly, sections of corals sampled for the Landsberg et al. (2020) paper had a fragment collected for light microscopy and from that fragment, a smaller (<5 mm) subfragment was fixed for TEM. So, the coral samples examined here were the same ones used to describe SCTLD by light microscopy in Landsberg et al. (2020; **Supplementary Table 1**). For methods of routine paraffin-embedded tissue sections with hematoxylin and eosin staining, refer to Landsberg et al. (2020). Briefly, a sample targeted for TEM (less than 0.5 cm diameter) to encompass surface and portions of basal body wall was excised with a bone cutter from a piece of core biopsy punch (2.54 cm diameter size) taken for histology, and live tissues placed in TEM fixative. Fragments were labeled as originating from apparently healthy colonies (Healthy) originating from geographic areas not then known to have SCTLD based on absence of gross lesions [see Landsberg et al. (2020) for details], or colonies manifesting gross lesions of SCTLD comprising apparently normal fragments (SCTLD-Healthy) or fragments with lesions (SCTLD-Lesion). For SCTLD-Lesion, sampling focused on intact tissue or areas with apparent tissue integrity near bare skeleton. Fragments were stored at 4°C in TEM fixative until processing.

To prepare fragments for TEM examination in the United States Geological Survey, National Wildlife Health Center, Honolulu Field Station, corals were decalcified in 10% EDTA (1–2 days) then postfixed in TEM fixative. Tissues were then rinsed in 0.1 M sodium cacodylate buffer containing 0.35 M sucrose and postfixed with 1% osmium tetroxide in 0.1 M sodium cacodylate buffer. Tissue was dehydrated in a graded ethanol series, the ethanol was replaced with propylene oxide, and the tissue was embedded in LX112 epoxy resin. Epoxy-embedded tissues were cut into 1-μm thick sections and stained with Richardson's stain for light microscopy. For electron microscopy, ultrathin (60- to 80-nm) sections were obtained on an RMC Powertome ultramicrotome, double stained with uranyl acetate and lead citrate, viewed on a Hitachi HT7700 transmission electron microscope at 100 kV, and photographed with an AMT XR-41B 2k-by-2k charge-coupled device camera.

To prepare fragments for TEM examination in Florida, samples were decalcified with 10% EDTA solution for 8 days without agarose enrobing, followed by postfixation with 1% osmium tetroxide in 1.25% sodium bicarbonate buffer, pH 7.2, for 1 h at room temperature. Tissue samples were then washed in Nano-pure water, three times, for 5 min each, and subsequently dehydrated in a graded series of ethanols and embedded in Spurr's epoxy resin. Thin sections (90 nm) were cut with a diamond knife on a Leica EM UC6 ultramicrotome and placed on grids. The sections were post-stained with 2% uranyl acetate in 50% ethanol and Reynolds' lead citrate (Reynolds, 1963) and examined with a Jeol JEM-1400 transmission electron microscope in TEM bright field mode at 80 kV.

The tissues of surface body wall (epidermis, mesoglea, gastrodermis with endosymbionts) and basal body wall (gastrodermis with endosymbionts, mesoglea, calicodermis) were examined and representative lesions were photographed. Coral host cells and symbionts were judged healthy if they had intact cell and nuclear membranes with expected complement of organelles or structures appropriate to that cell type (Fautin and Mariscal, 1991).

During examination of tissues, it became evident, based on variety of pathology in endosymbionts, that efforts be dedicated to documenting morphologic changes in endosymbionts that differed from what has been described for normal endosymbionts in the literature. Normal endosymbionts (Trench and Blank, 1987; Wakefield et al., 2000) enclosed by a host symbiosome membrane are characterized by a cell wall enclosing a space mostly filled by a peripherally located multi-lobed chloroplast composed of stacked thylakoid membranes, a stalked pyrenoid surrounded by an annulus of starch, a nucleus with condensed chromatin, mitochondria, starch granules, lipid vacuoles, and sometimes a granular accumulation body (**Figure 1A**). The following features were categorized as present/absent in the first 30 endosymbionts encountered on a TEM grid for each sample, because they were morphologic changes that deviate from what is considered normal endosymbionts ultrastructure (Trench and Blank, 1987; Wakefield et al., 2000): loss of laminar detail in thylakoid membranes, gigantism of chloroplast exemplified by enlarged chloroplasts with remnants of thylakoid membranes, absence of starch granules, absence of annular starch around pyrenoid (**Figure 1B**), presence of amorphous homogenous electron-dense aggregates in endosymbiont cytoplasm or membrane formation within intracellular cavities (**Figure 1C**), presence of variably sized non-membrane bound cavities within the cell cytoplasm (**Figures 1C–E**), and lysis of endosymbionts. We also categorized anisometric viral-like particles (AVLP) compatible in morphology and size with positive single-stranded RNA (+ssRNA) viruses of plants with linear to sinuous morphology (Stevens, 1983; Agrios, 2004) as follows: whorled electron-dense material (viroplasm; **Figure 1E**) often associated with fine AVLP (**Figures 1F**, **2A,B**), coarse AVLP arranged in stellate clusters (**Figures 2C,D**), or coarse AVLP in layered or haphazard clusters (**Figures 2E,F**; Zechmann and Zellnig, 2009). Mucus in coral tissues was identified in TEMs according to published criteria (Fautin and Mariscal, 1991). Representative photographs were also taken of endosymbionts to document features listed above. For negative stains, fixed tissues were macerated into a slurry that was placed on a TEM grid, stained with ca. 1% uranyl acetate, and imaged as above.

We processed 25 samples of five coral species including six samples each from *M. cavernosa* and *Pseudodiploria strigosa*, five each from *Colpophyllia natans* and *Orbicella faveolata*, and three from *Siderastrea siderea* comprising 11 SCTLD-Healthy, 9 SCTLD-Lesion, and 5 Healthy from a reference area, outside of known SCTLD locations at the time of sampling (Landsberg et al., 2020). The total number of individual colonies examined for TEM was 19. Additional 2016 archived TEM samples of two *M. cavernosa* were reviewed for potential presence of AVLP and pathological changes in endosymbionts. 1776

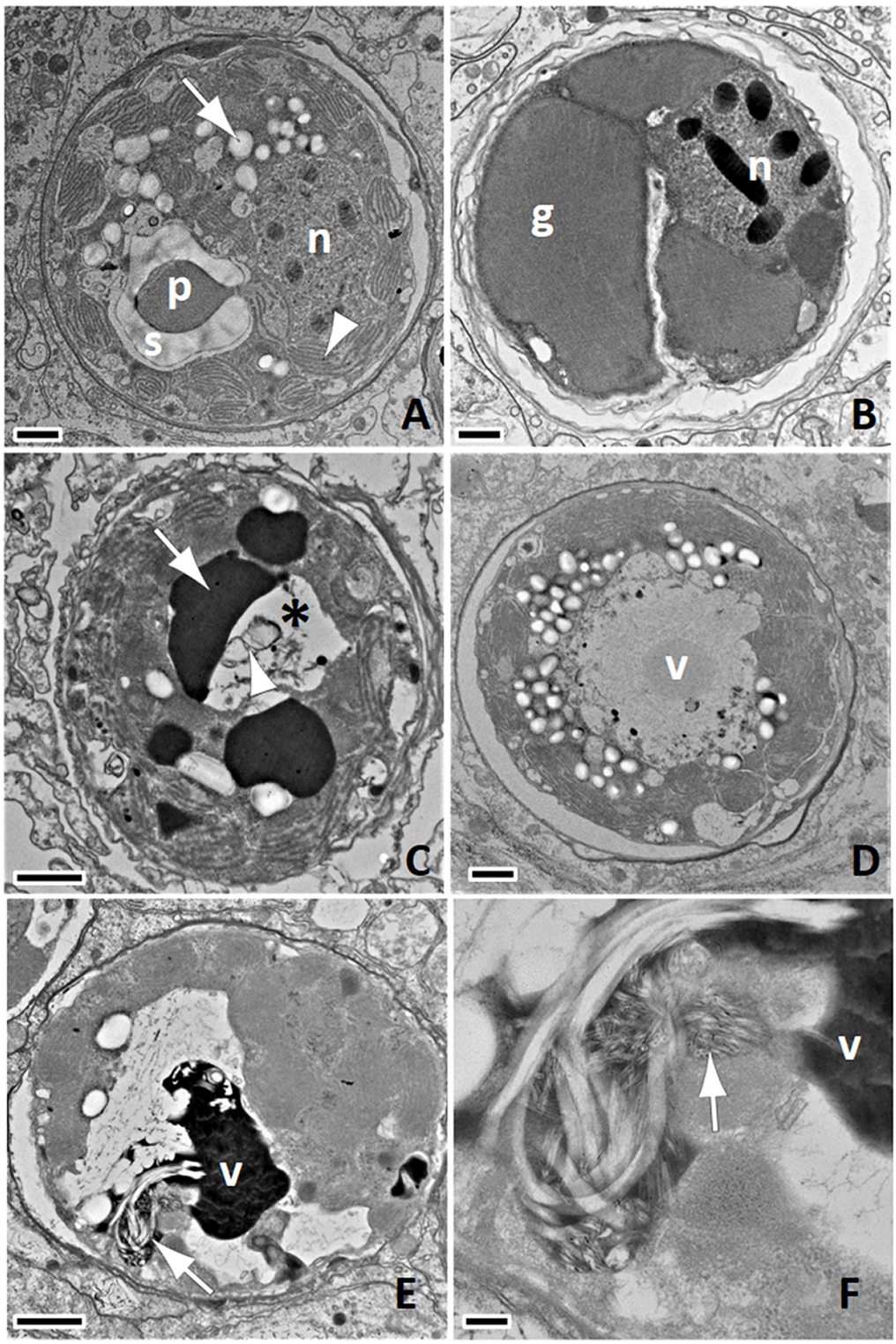

FIGURE 1 | (A) Normal endosymbiont with pyrenoid (p) and annular starch (s), starch granule (white arrow), nucleus (n), multilobulated chloroplasts with distinct thylakoid membranes (arrowhead); bar = 1 μm, *S. siderea* SCTLD-Healthy. **(B)** Gigantism of chloroplasts (g); note massive enlargement and lack of detail of thylakoid membranes, lack of starch granules, and lack of pyrenoid with nucleus (n); bar = 1 μm, *M. cavernosa* SCTLD-Healthy. **(C)** Cavity (asterisk) and electron-dense amorphous matrix (arrow) and membrane formation (arrowhead); bar = 1 μm, *P. strigosa* SCTLD-Healthy. **(D)** Cavity with viroplasm (v) from which emanate coarse anisometric viral-like particles (AVLP), the granular material surrounding the viroplasm; bar = 1 μm, *O. faveolata* SCTLD-Healthy. **(E)** Whorled electron-dense viroplasm (v) and AVLP (arrow) within cavity; bar = 1 μm, *P. strigosa* SCTLD-Lesion, **(F)** Detail of **(E)** note putative early stage AVLP (arrow) near viroplasm (v); bar = 200 nm.

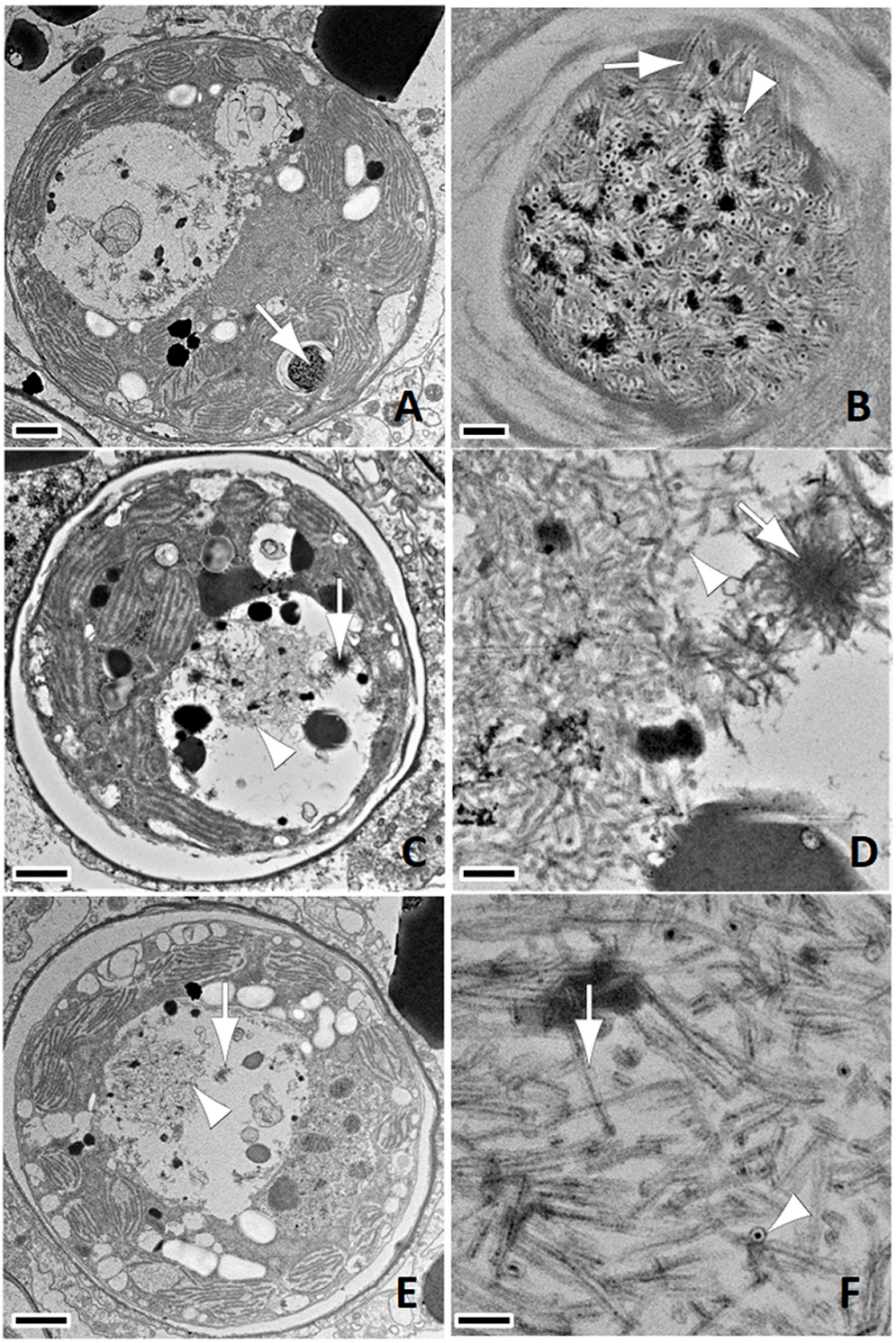

FIGURE 2 | (A) Endosymbiont with intracellular cavity and putative early inclusion of anisometric viral-like particles (AVLP) within chloroplasts (arrow); bar = 1 μm, *C. natans* SCTLD-Lesion. **(B)** Detail of **(A)**; note arrays of sinuous AVLP (arrow) mixed with electron-dense material and cross sections with a core (arrowhead); bar = 100 nm. **(C)** Putative intermediate stage of viral infection; note large cavity containing clumps of electron-dense material and clusters of coarse AVLP arranged in stellate (arrow) and haphazard (arrowhead) pattern; bar = 1 μm, *O. faveolata* SCTLD-Healthy. **(D)** Detail of **(C)**; note cluster of stellate AVLP (arrow) and coarser haphazardly arranged AVLP (arrowhead) admixed with clumps of electron-dense material; bar = 200 nm. **(E)** Putative advanced stage of viral infection; note cavity containing clumps of electron-dense material mixed with AVLP arranged in stellate (arrow) or haphazard manner (arrowhead); bar = 1 μm, *C. natans* SCTLD-Healthy. **(F)** Detail of haphazardly arranged AVLP; note core in sagittal (arrow) of AVLP apparently emanating from electron-dense viroplasm and cross (arrowhead) sections of individual AVLP; bar = 100 nm.

TABLE 1 | Number of TEM photomicrographs (number of individual endosymbionts) partitioned by health status of fragment and genus.

Genus	SCTLD-lesion	SCTLD-healthy	Healthy	Grand total
Colpophyllia natans	136 (52)	152 (12)	20 (76)	308 (140)
Montastraea cavernosa	100 (37)	202 (29)	60 (78)	362 (144)
Orbicella faveolata	105 (26)	152 (29)	87 (55)	344 (110)
Pseudodiploria strigosa	136 (63)	181 (21)	60 (67)	377 (151)
Siderastrea siderea	126 (33)	73 (47)	186 (19)	385 (99)
Grand total	603 (211)	760 (138)	413 (295)	1,776 (644)

photographs comprising 644 endosymbionts were also taken to document features (**Table 1**). Features were enumerated in 735 endosymbionts (only 15 endosymbionts were seen in one sample). This number differs from the 644 endosymbionts photographed in that we did not photograph every endosymbiont seen. A pairwise scatterplot of all ten pathological features described above along with correlation coefficients were plotted and analyzed for all corals regardless of health status. All analyses were done with R (R Core Team, 2017).

RESULTS

Putative Viral Infections

Putative early viral infections were inferred as such based on the size of viral inclusions. This assumed that smaller inclusions most often associated with viroplasm (assembly components of viruses) were early stages and larger inclusions less often associated with viroplasm were likely later stages (McWhorter, 1965). In this study, putative early viral inclusions were characterized by clumps of electron-dense whorls associated with fine AVLP (**Figures 1E,F**, **2A,B**). Putative intermediate stage viral infections were characterized by AVLP arrayed in haphazard or stellate patterns and found almost exclusively in cavities within endosymbionts (**Figures 2C,D**). AVLP were occasionally associated with electron-dense to stippled viroplasm (**Figure 3A**) and more often with stacked or laminated membranes (**Figure 3B**). Membranes were also evident, associated with stippled viroplasm (**Figures 3C,D**). Putative late-stage infections were characterized by large cavities replete with coarse AVLP (**Figures 2E,F**) that occasionally appeared to originate from electron-dense viroplasms (**Figures 3E,F**); AVLP ranged in diameter from 15–20 nm. Terminal infections were characterized by endosymbionts distorted with large cavities replete with stacks of coarse AVLP mixed with membranes (**Figures 4A,B**) or clusters of AVLP that appeared to be emerging from host cells associated with lysed cell membrane (**Figures 4C–F**). Fifteen/735 (2%) enumerated endosymbionts were lysed. Negative stains revealed sinuous (**Figure 5A**) to linear (**Figure 5B**) filamentous AVLP ranging in width from 18 to 20 nm and length from 558 to 6,697 nm. Like the 2018 samples, we also confirmed putative AVLP in TEMs of endosymbionts prepared from archived lesioned *M. cavernosa* samples obtained in July and November 2016 from the Upper Keys (Grecian Rocks) and Southeast Florida (Broward County 4), respectively, (Landsberg et al., 2020) with associated chloroplast pathology exemplified by AVLP associated with membrane-bound vesicle formation in chloroplasts, and degrading thylakoid lamellae (**Supplementary Figure 1**). AVLP appeared limited to endosymbiont cytoplasm with apparent early stages (smaller aggregates of AVLP) associated with the chloroplast and later stages seen in cavities in degrading endosymbionts adjacent to deformed chloroplasts (**Figures 1–5** and **Supplementary Figures 1E,F**).

Endosymbiont Pathology

Intracellular cavities and shrinkage of endosymbionts within symbiosomes were the only changes we could reliably relate from light microscopy to TEM. On light microscopy, cavities were variably sized and differentiated from pyrenoids that have a distinct core and annulus (**Figure 5C**). Putative inclusions or viroplasm (**Figures 5C–E**) were inferred on light microscopy by their punctate refractile appearance. Shrunken endosymbionts were characterized by hypereosinophilic cytoplasm and increased space in the symbiosomes (**Figures 5C,F**). In addition to aforementioned changes in starch or chloroplasts, we occasionally saw accumulations of what appeared to be stacks of scrolled cell membranes accumulating in the enlarged symbiosome spaces (**Figures 6A,B**).

Coral Host Cell Pathology

The most significant aspect of coral host cell pathology was hyperplasia and hypertrophy of mucocytes in the gastrodermis leading to general effacement of tissue architecture with swollen mucocytes and ruptured cell membranes visible with both light microscopy (**Figure 6C**) and TEM (**Figures 6D–F**). On TEM images, putative early changes consisted of localized swelling of mucocytes (**Figure 6D**) that appeared to progress to general cell distention accompanied by rupture of cell membranes with accumulations of cell debris underlying mesoglea and leading to separation of calicodermis (**Figure 6E**). Putative late-stage (more severe) changes were characterized by massive deposits of mucus effacing tissue architecture of gastrodermis, liberation of endosymbionts into gastrovascular canals, and accumulations of debris in mesoglea separating calicodermis from gastrodermis (**Figure 6F**). Nuclei of gastrodermal cells with symbiosomes appeared uniformly intact.

Quantification of Endosymbiont Pathology

Of the ten morphologic changes enumerated from most to least common were absence of annular starch granule around pyrenoid (448/735 or 61%), electron-dense bodies (416/735 or 56%), variably sized intracellular cavity (400/735 or 54% each), indistinct thylakoid membrane (324/735 or 44%), stellate AVLP (282/735 or 38%), membrane formation (180/735 or 24%), absence of starch granules (139/735 or 19%), fine AVLP (120/735 or 16%), gigantism of chloroplasts (93/735 or13%), and coarse AVLP (49/735 or 7%).

All morphologic changes were observed and photographed in all species regardless of health status. For enumerated

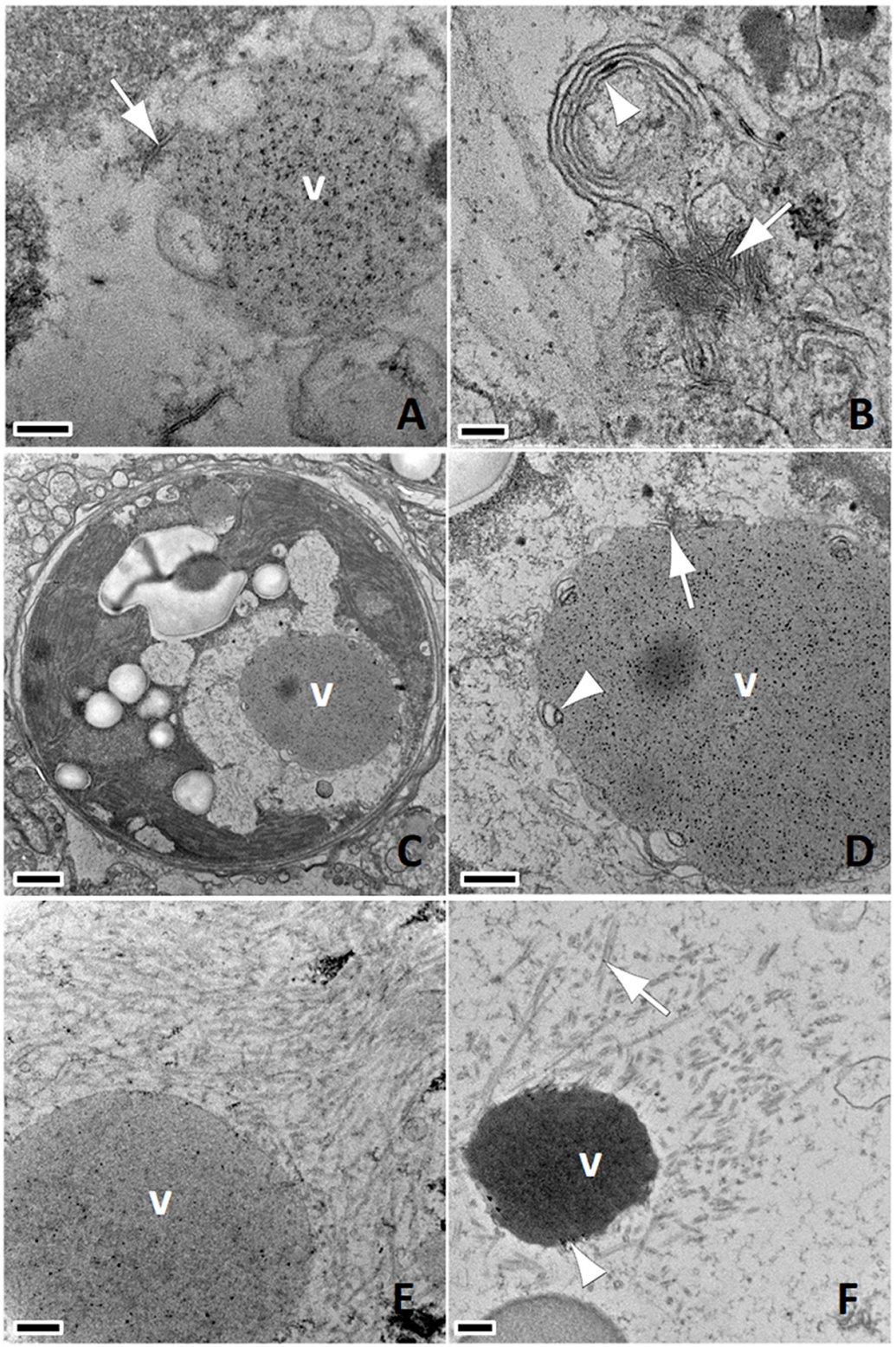

FIGURE 3 | (A) Note detail of viroplasm (v) with formation of anisometric viral-like particle (AVLP-arrow); bar = 100 nm, *C. natans* SCTLD-Healthy. **(B)** Note laminated membranes (arrowhead) associated with cluster arranged stellate AVLP (arrow); bar = 100 nm, *M. cavernosa* SCTLD-Healthy. **(C)** Note large cavity with electron-dense material suggestive of viroplasm (v); bar = 1 μm, *C. natans* SCTLD-Lesion. **(D)** Close up of **(A)** with viroplasm (v), cluster of stellate AVLP (arrow), and membrane formation (arrowhead); bar = 400 nm. **(E)** Note viroplasm (v) surrounded by numerous haphazardly arranged coarse AVLP; bar = 200 nm, *C. natans* SCTLD-Healthy. **(F)** More electron-dense viroplasm (v) out of which appear to arise AVLP visible in longitudinal (arrow) and cross (arrowhead) sections; bar = 200 nm, *C. natans* SCTLD-Healthy.

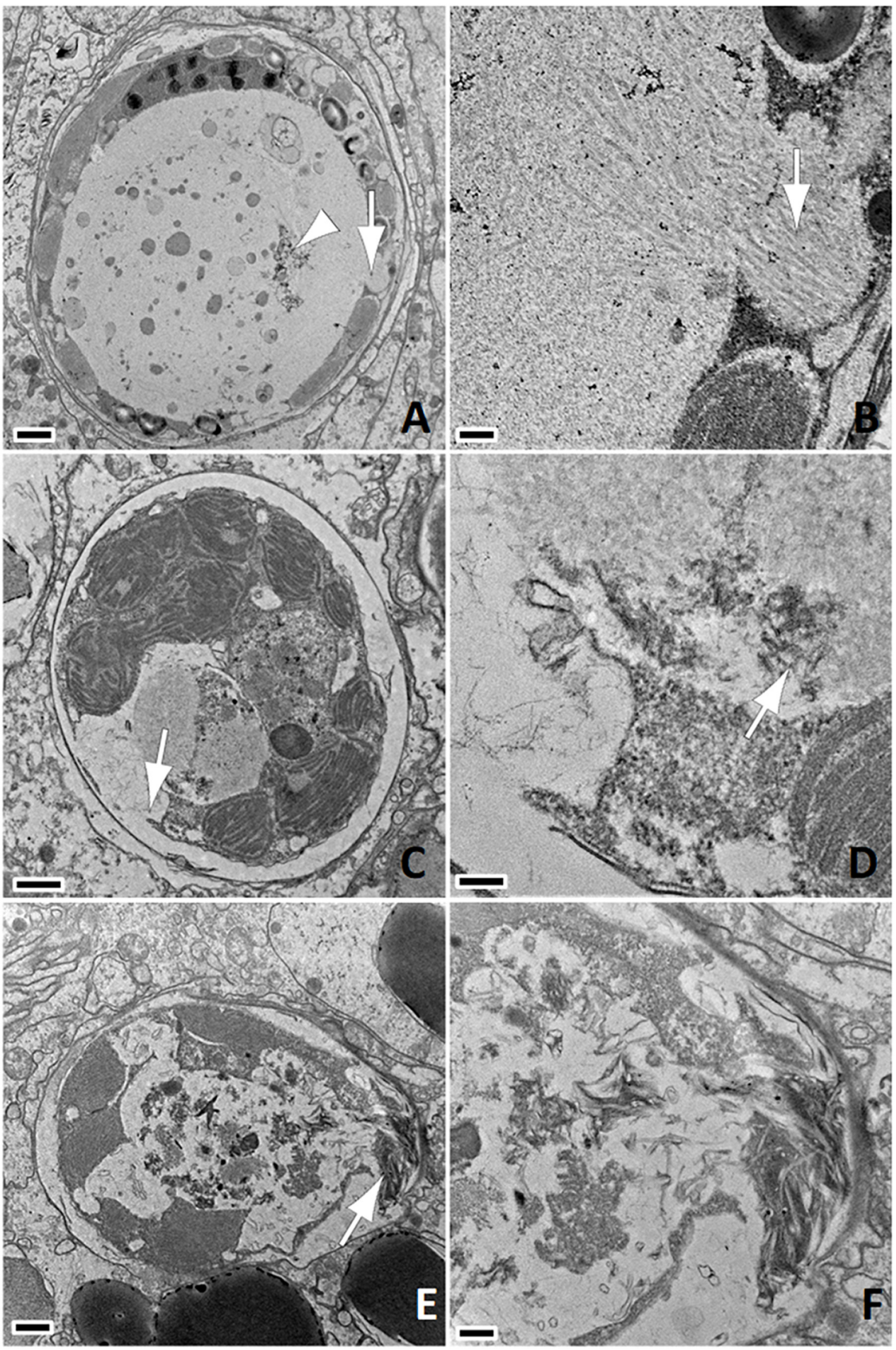

FIGURE 4 | (A) Putative late-stage infection; note large cavity effacing most of the cellular architecture and replete with electron-dense material, membranes (arrowhead) and anisometric viral-like particles (AVLP, arrow); bar = 1 μm, *M. cavernosa* SCTLD-Healthy. **(B)** Detail of **(A)**; note AVLP arrayed in lamina (arrow); bar = 200 nm. **(C)** Large inclusion of coarse AVLP arrayed haphazardly mixed with electron-dense material associated with lysis of cell wall (arrow); bar = 1 μm, *P. strigosa* SCTLD-Healthy. **(D)** Detail of **(C)**; note AVLP (arrow) near lysed cell wall to the left; bar = 200 nm. **(E)** Lysed cell; note large pleomorphic cavity with abundant debris and loss of membrane integrity with clumps of AVLP (arrow); bar = 1 μm, *P. strigosa* SCTLD-Healthy. **(F)** Detail of **(E)**; bar = 500 nm.

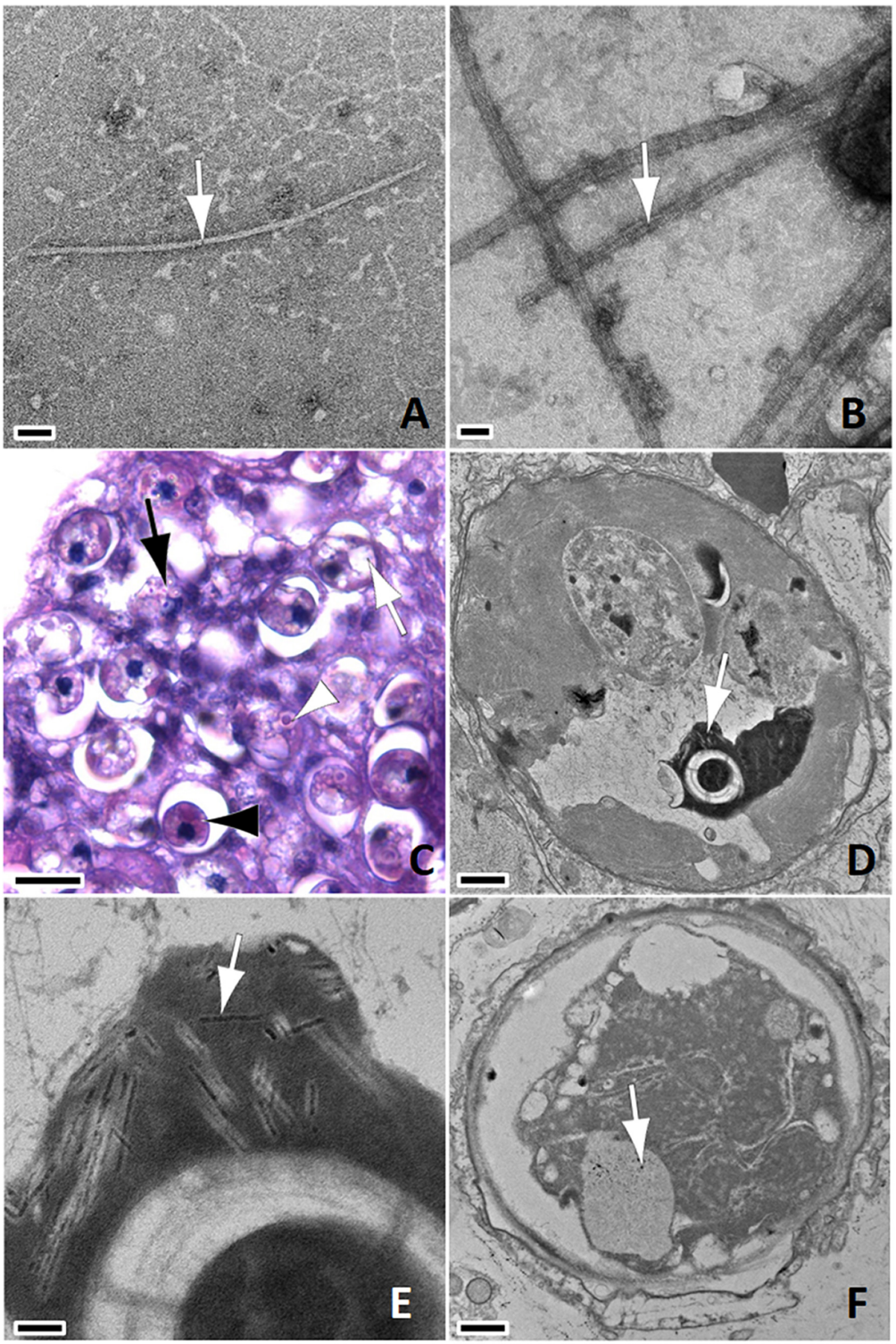

FIGURE 5 | (A) Linear anisometric viral-like particles (AVLP -arrow); negative stain; bar = 200 nm, *P. strigosa* SCTLD-Lesion. **(B)** Linear AVLP with electron-dense core (arrow); negative stain; bar = 50 nm, *P. strigosa* SCTLD-Lesion. **(C)** Light micrograph of paraffin embedded section. Note endosymbionts with pyrenoid (white arrowhead) characterized by eosinophilic core surrounded by lighter annulus, intracellular cavity (white arrow), putative viroplasm or early inclusions with punctate refractile appearance (black arrow), and shrunken endosymbiont with hypereosinophilic cytoplasm (black arrowhead); H&E; bar = 10 μm, *M. cavernosa* SCTLD-Lesion. **(D)** TEM of endosymbiont with cavity containing whorled viroplasm (arrow); 800 nm, *P. strigosa* SCTLD-Lesion. **(E)** Close up of **(D)**; note AVLP in various stages of formation (arrow) within viroplasm; bar = 100 nm. **(F)** Shrunken endosymbiont within symbiosome; note deformed cell wall, absence of pyrenoid, starch granules, loss of detail of thylakoid membranes, and aggregate of coarse AVLP within chloroplast (arrow); bar = 1 μm, *C. natans* SCTLD-Healthy.

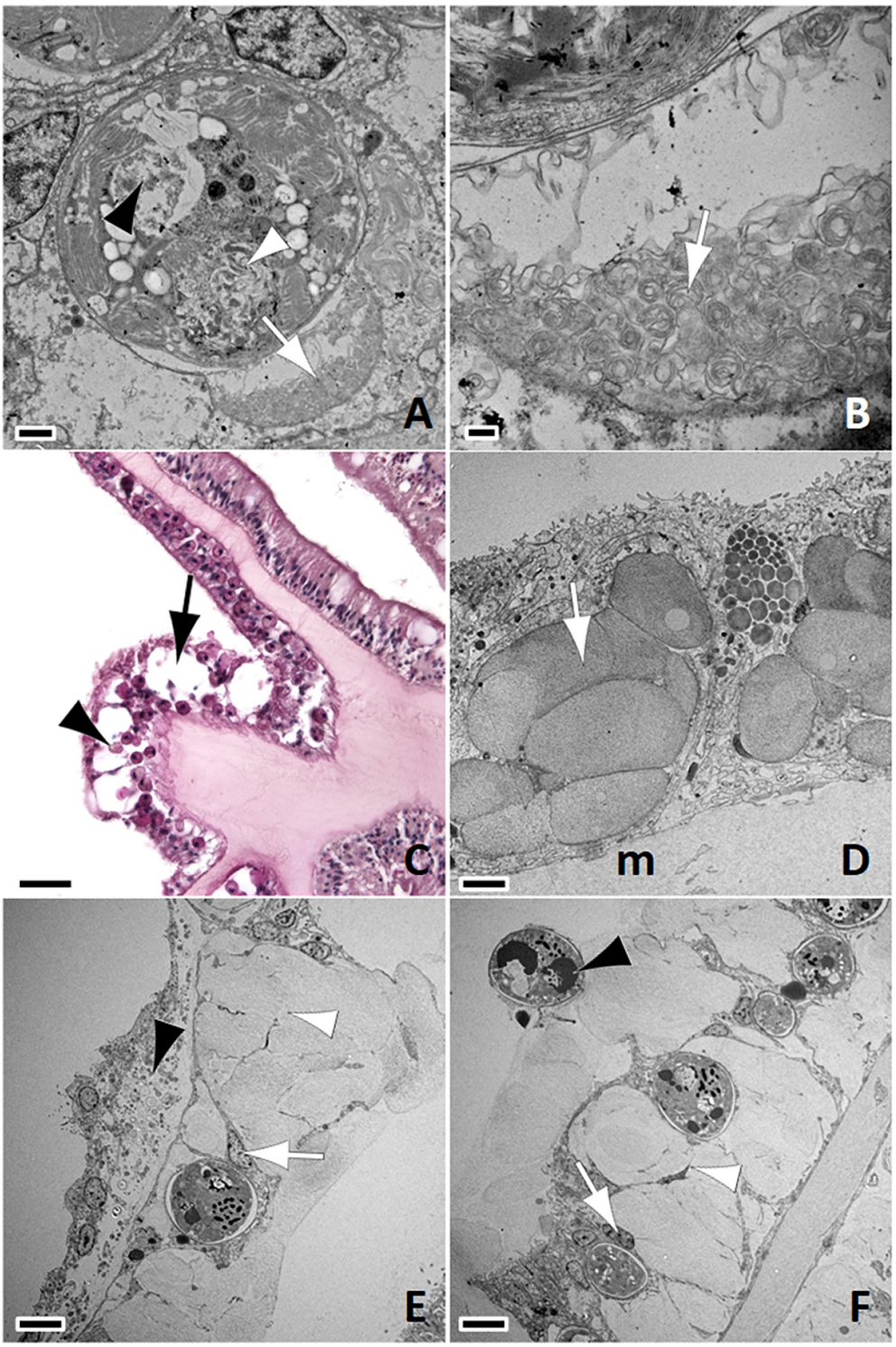

FIGURE 6 | (A) Endosymbiont with cavity (black arrowhead), viroplasm (white arrowhead), and accumulation of scrolled membranes within symbiosome (arrow); bar = 1 μm, *S. siderea* Healthy. **(B)** Detail of **(A)**; note accumulations of scrolled membranes (arrow); bar = 200 nm. **(C)** Light micrograph of paraffin embedded section. Note swelling of gastrodermis (arrow) with liberation of endosymbionts (arrowhead); H&E; bar = 50 μm, *S. siderea* SCTLD-Lesion. **(D)** Note putative early stage lesion with swollen mucocytes (arrow) among gastrodermal cells overlying mesoglea (m); bar = 4 μm, *C. natans* SCTLD-Lesion. **(E)** Note putative intermediate-to-late-stage lesion with markedly swollen mucocytes disrupting cellular architecture with rupture of cell membranes (white arrowhead), debris in mesoglea with lifting off of calicodermis (black arrowhead), and endosymbiont within gastrodermal cell with intact nucleus (white arrow); Skeleton to left, gastrovascular canal to right. bar = 6 μm, *O. faveolata* SCTLD-Healthy. **(F)** Note massive mucus production disrupting gastrodermal architecture with cell membrane rupture (white arrowhead), mucus secretions in the gastrovascular canals along with an endosymbiont (black arrowhead), and endosymbionts within gastrodermal cells with intact nuclei enclosed by symbiosomes (white arrow); bar = 6 μm, *O. faveolata* SCTLD-Healthy.

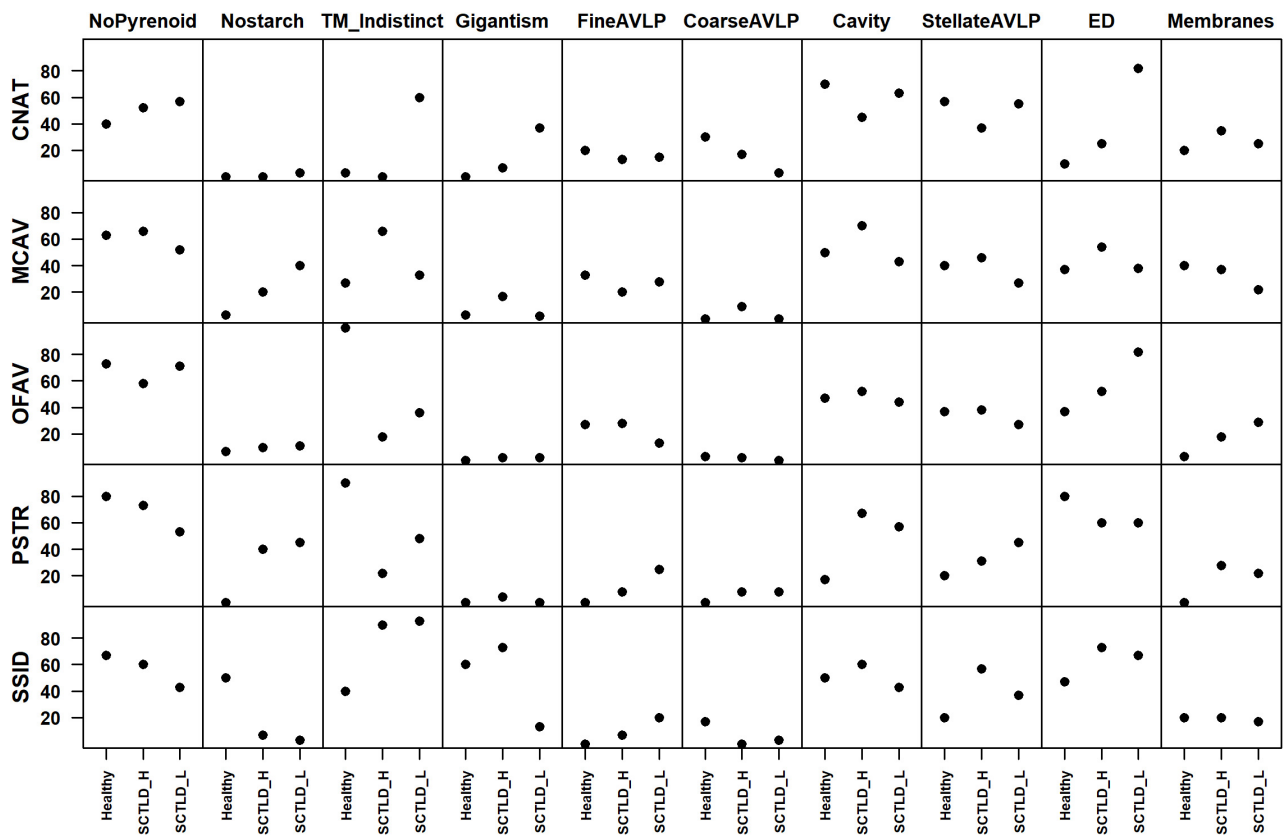

FIGURE 7 | Percent of endosymbionts enumerated manifesting various morphologic abnormalities partitioned by abnormalities, health status, and species. CNAT-*C. natans*, MCAV-*M. cavernosa*, OFAV-*O. faveolata*, PRST-*P. strigosa*, and SSID-*S. siderea*. For features, ED stands for electron dense bodies, TM_Indistinct stands for indistinct thylakoid membrane, and AVLP stands for anisometric viral-like particle. For *X* axis, SCTLD_H and SCTLD-L stand for healthy and lesion fragments from SCTLD affected corals, respectively.

endosymbionts, fine AVLP were seen in 0–33% of endosymbionts in each of the samples whereas coarse AVLP were seen in 0–30%. Intracellular cavities were seen in 17–70% endosymbionts in each of the samples whereas stellate AVLP were seen in 20–57%. Electron-dense bodies were seen in 10–82% of the endosymbionts in each of the samples whereas membranes were seen in 0–40%. Missing circumpyrenoid starch annulus was seen in 40–80% of the endosymbionts in each of the samples whereas missing starch granules were seen in 0–50%. Indistinct thylakoid membranes were seen in 0–100% of the endosymbionts in each of the samples whereas gigantism was seen in 0–73%. No consistent pattern was seen across species or health condition for any of these features (**Supplementary Table 2** and **Figure 7**). The highest correlation coefficients between pathology features across species and health states were those between stellate AVLP and cavity formation and those between electron dense bodies and coarse AVLP (**Supplementary Figure 2**).

DISCUSSION

Ultrastructural morphologic changes in Florida corals affected with SCTLD and apparently healthy corals seen here were suggestive of a viral infection affecting exclusively their endosymbionts. Unlike cases of bleaching, or white syndrome, where viral-like particles (VLPs) have been documented in coral host tissues (Patten et al., 2008; Bettarel et al., 2013), we did not see AVLP in coral host cells. Rather, abnormalities in coral host cells were initially limited to mucus hyperplasia/hypertrophy. In apparently early stages of SCTLD where endosymbionts contained mild pathology such as small AVLP inclusions and small cavities, coral host cells enclosing the endosymbionts were intact with healthy-appearing nuclei and the expected complement of internal organelles (**Figures 6E,F**). This indicates that SCTLD is, fundamentally, a disease of the endosymbionts that eventually leads to coral host cell death.

Three lines of evidence point to +ssRNA viruses as an explanation for the presence of AVLP in endosymbionts. First, all known viruses of plants with filamentous to linear morphology are +ssRNA viruses (Agrios, 2004; Martelli et al., 2007). Second, +ssRNA viruses promote membrane formation in host cells, because these membranes are used by virally encoded proteins to make -ssRNA that is then used as a template to make +ssRNA (Ahlquist, 2006; Martelli et al., 2007), and membrane formation was a prominent feature of endosymbiont pathology. Third, +ssRNA viruses replicate in cell cytoplasm and do not bud from

the host cell membrane (Ahlquist, 2006), a consistent feature of endosymbionts seen here where AVLP were exclusively located in the cytoplasm either in or near chloroplasts in early stages or more commonly in cavities adjacent to chloroplasts.

Negative stains confirmed the filamentous nature of AVLP with dimensions compatible with those of +ssRNA viruses that in plants range from 10 to 28 nm wide and 128–1,250 nm long with a filamentous core (Stevens, 1983). This group of viruses are classified as Flexiviridae (Martelli et al., 2007). We acknowledge that some of the AVLP seen in negative stains here were up to five times as long as the longest known plant Flexivirus, and possibly not all AVLP seen on negative stain were actual viruses. The only linear structures we are aware of in corals are collagen fibers and nematocysts tubules. The AVLP on negative stain were too narrow to be nematocysts' tubules that exceed 300 nm diameter (Reft, 2012). Likewise, the AVLP on negative stain were unlike collagen fibrils that have distinct striations, do not have a core, and generally have a diameter exceeding 30 nm (Starborg et al., 2013). Future efforts to confirm dimensions of AVLP by virus isolation attempts or immunogold studies to tag confirmed viruses would be important areas to pursue.

Two explanations exist for the different morphologies of AVLP seen here: (1) Endosymbionts, the species of which we were unable to identify by ultrastructure, are infected with at least three different types of viruses or, (2) This variation in morphology reflects different developmental forms of the same virus. As the most parsimonious explanation, we suspect the second option is more likely. In animals (Netherton et al., 2007) and plants (Yang et al., 2017), virus particle assembly goes through a maturation process involving nucleic acids and proteins that are initially visible as amorphous electron-dense masses (viroplasm) from which emerge mature viral particles. This pattern was evident in multiple endosymbionts from multiple corals. We inferred the progression of early- versus late-stage virus disease based on the size of viral inclusions, assuming that smaller inclusions most often associated with viroplasm (assembly components of viruses) were early stages and larger inclusions less often associated with viroplasm were likely later stages (McWhorter, 1965).

Morphologic changes in host endosymbionts including formation of variably sized intracellular cavities, loss of detail of thylakoid membranes and gigantism of chloroplasts (**Figure 7**) were also compatible with the way these organelles respond to virus infections in plants. In plants, the chloroplast is often targeted by viruses (Zhao et al., 2016; Bhattacharyya and Chakraborty, 2018; Jin et al., 2018), and virus-infected chloroplasts manifest morphologic changes very similar to those seen in endosymbionts here. For example, during the +ssRNA (barley stripe mosaic virus) infection and viral replication complex formation, chloroplast abnormalities included the formation of peripheral vesicles and cytoplasmic invaginations (Jin et al., 2018), with the former notably observed in early stage chloroplast degradation associated with putative VLPs in *M. cavernosa* endosymbionts (**Supplementary Figure 1**). Given that the chloroplast makes up a considerable volume of the endosymbiont, this organelle could be a primary target for viral infections. Other changes such as loss of starch seen in endosymbionts were less clearly associated with viral infections. Electron-dense structures in cavities within endosymbionts could have been lipids (Weng et al., 2014) or viroplasm.

Cavities in endosymbionts were round and often filled with debris but were unlike accumulation bodies. Accumulation bodies in endosymbionts, hypothesized to be waste accumulation structures, are normally round and filled with tightly packed electron-dense material (Taylor, 1968; Zhu et al., 2011). In contrast, in endosymbionts examined here, cavities were correlated with presence of AVLP (**Supplementary Figure 2**) mixed with debris, electron-lucent matrix, membranes, and viroplasm. Finally, depletion of starch reserves was commonly seen indicating depletion of energy reserves or inability of the cell to generate sugars. This would accord with chloroplast pathology, which likely resulted in reduced ability of the cell to carry out photosynthesis, a key process needed to generate sugars in endosymbionts (Yellowlees et al., 2008). Reduced photosynthesis can lead to starch depletion in endosymbionts in other Cnidaria. For instance, light-starved *Aiptasia* have endosymbionts with reduced starch reserves (Muller-Parker et al., 1996). Whether the cavities were a harbinger of endosymbiont death could not be confirmed from findings herein. In plants, vacuolation is an important morphologic indicator of cell death (van Doorn et al., 2011), however, we were unable to convincingly see membranes surrounding the intracellular spaces of endosymbionts, and thus termed them cavities. Clearly, lysed endosymbionts were likely dead. Ideally, documenting morphologic progression of endosymbiont pathology associated with AVLP in more controlled settings, preferably with cultured endosymbionts, would help clarify pathogenesis of this disease.

Viruses have been detected in corals by electron microscopy and molecular assays, and they are thought to play potentially important roles in coral bleaching, stress responses, and microbial turnover (Vega Thurber and Correa, 2011). In free-living marine phytoplankton, including dinoflagellates, double-stranded icosahedral DNA viruses in the Phycodnaviridae are well known but in recent years, evidence for a significant ecological role of +ssRNA viruses has been found (Nagasaki et al., 2006). For example, the icosahedral + ssRNA virus, HcRNAV (*Alternavirdiae*, dinornavirus) plays a major role in the termination of *Heterocapsa circularisquama* blooms through lytic activity (Tomaru and Nagasaki, 2004; Tomaru et al., 2007). Viral lysis of dinoflagellate endosymbionts has also been explored as one possible mechanism for coral bleaching. A small (∼30 nm diameter) icosahedral ssRNA virus closely related to HcRNAV and the cricket paralysis virus have been detected in coral-associated endosymbionts (Correa et al., 2013, 2016; Levin et al., 2017; Montalvo-Proaño et al., 2017; Grupstra et al., 2021), but pathogenic mechanisms for these endosymbiont viruses in coral diseases have yet to be systematically proven. Endosymbionts are hosts for a diverse assemblage of viruses, mainly double stranded DNA bacteriophages, which may not necessarily be pathogenic (van Oppen et al., 2009; Wood-Charlson et al., 2015). Molecular assays detect only the presence of an infectious agent and by themselves provide little information as to the viability of the agent or its role in causing host cell pathology and disease. Putative pathogenicity of an infectious agent to a

host can only be reliably determined by documenting host cell pathology associated with that agent (Work and Meteyer, 2014), as in this study.

Uncharacterized VLPs have been extensively documented in endosymbionts by electron microscopy both in hospite and culture. For instance, VLP were seen in thylakoids of endosymbionts from heat-shocked *Anemonia viridis* (Wilson et al., 2001), in UV-treated endosymbionts cultures (Lawrence et al., 2014), and VLP were seen in host tissues and endosymbionts of heat-shocked *Pavona danai* (Wilson et al., 2005). Various morphologies of VLP were seen in mucus of *Pseudodiploria* and *Acropora* from Australia (Davy and Patten, 2007), water surrounding thermally stressed endosymbionts (Davy et al., 2006), and within endosymbionts of heat-stressed *P. damicornis* (Grupstra et al., 2021). Unfortunately, in these studies, VLP were sparse, making them very difficult to differentiate from similar sized and shaped structures that often turn out to be artifacts such as condensed proteins or nucleic acids, a common problem in interpretation of transmission electron micrographs (Ackermann and Tiekotter, 2012). Moreover, none of these studies showed convincing morphologic evidence of cell pathology associated with viral infection; however, we acknowledge that these studies did not have as a primary objective to document host cell pathology associated with viral replication. Ideally, documentation of plausible viral infections in organisms by TEM should illustrate various stages of viral morphogenesis associated with clear evidence of cell pathology with abundant virions (Work et al., 2017). It is these aspects of our findings and their consistency across susceptible sampled species that make a compelling case for the possibility that a lethal viral infection of endosymbionts could be involved in the pathogenesis of SCTLD. That said, confirming the role of AVLP in causing lesions seen in endosymbionts will benefit from additional studies, ideally such as virus isolation in cultured cells so that progression of morphologic changes associated with viral infection over time can be more closely monitored.

Another interpretation of our findings is that the AVLP seen in chloroplasts are some form of degradation structures of this organelle (e.g., thylakoid membranes) secondary to heat stress or other undefined environmental insult. Structures observed here have not been documented by TEM in endosymbionts of *E. paradivisa* exposed to particulate organic matter (Rosset et al., 2015), *Aiptasia pallida* deprived of light (Muller-Parker et al., 1996), *A. digitifera*, *E. hirsutissima*, *P. rus*, *P. damicornis*, and *Aiptasia pulchella* undergoing bleaching (Ladrière et al., 2008), *A. pulchella* undergoing nitrogen deprivation (Jiang et al., 2014), or *P. damicornis* exposed to UV and far-red radiation (Camaya et al., 2016). The three exceptions were studies on endosymbionts from unspecified Cnidaria by Lohr et al. (2007), studies with *A. pulchella* by Lawrence et al. (2014), and studies with *A. tenuis* by Weynberg et al. (2017) where cultured endosymbionts from archived and cultured collections exposed to UV radiation or heat showed intracytoplasmic cavities in endosymbionts associated with AVLP. Interestingly, in the one study where molecular analyses were done, no sequences of Flexiviridae were seen (Weynberg et al., 2017). However, the genomes of Flexiviridae are not well conserved and can be very plastic (Martelli et al., 2007) perhaps making a divergent form hard to detect from existing genomic databases. Moreover, molecular detection of viruses from marine specimens can be a fraught endeavor subject to whims of methods of nucleic acid extraction, sample purification, and other procedural variables that can significantly impact downstream bioinformatics analyses (Wood-Charlson et al., 2015). In plants, AVLP are not a feature of chloroplast degradation except for viral infections (Sowden et al., 2017), so it is difficult to explain the structures we saw as a byproduct of UV or heat exposure in corals.

The most obvious coral host response to endosymbiont pathology appeared mainly limited to hyperplasia and hypertrophy of mucocytes leading to disruption and effacement of gastrodermal architecture with rupture of cell membranes. This feature accorded with light microscopy where cell lysis (lytic necrosis) secondary to massive mucus production is a signal histologic feature of SCTLD (Landsberg et al., 2020), and fits with some features of cell necrosis in animal cells that include plasma membrane rupture (Kroemer et al., 2009). Unlike Landsberg et al. (2020), we did not see coral host cell changes in *Montastraea* such as degraded nuclei or vacuolation which were possibly more advanced than those documented here. Tissue sections for TEM are very small, so it is possible that the sections we examined did not have those host cell responses. Likewise, Landsberg et al. (2020) did not note the mucus changes seen in this study. These discrepancies illustrate that further studies to better characterize host cell pathology relative to progressive stages of SCTLD would be useful.

One possible reason why affected corals produce excessive mucus might be the result of endosymbiont metabolic dysfunction. Viral infections of eukaryotic algae can have profound effects on host cell metabolism influencing, for example, lipid metabolism, photosynthesis, and sulfur metabolism (Jackson et al., 2021). Chloroplasts clearly manifested varying degrees of pathology, and this organelle provides carbohydrates to the coral host through photosynthesis (Yellowlees et al., 2008). Gigantism of chloroplasts was occasionally seen and starch granule depletion in endosymbionts was common indicating an inability to store carbohydrates. Coral mucus is a carbohydrate-rich substance subject to many regulatory pathways such as diet, use for defense, aid to feeding, and maintenance of microbiome (Brown and Bythell, 2005), so many opportunities exist to disrupt its production. Additionally, in *Montastraea* heat stress can lead to loss of endosymbionts associated with increased mucocytes (Piggot et al., 2009). As such, the mucus production observed in this study could also simply be a host stress response. Disintegration of mesoglea and dissociation of calicodermis would accord with gross clinical signs of tissue loss, a key clinical manifestation of SCTLD. The calicodermis is the cell layer that adheres coral tissue to skeleton (Hyman, 1940), so loss of that layer would mean loss of tissue anchorage (Drake et al., 2020).

A viral infection killing endosymbionts would explain many epidemiologic and anatomic features of SCTLD. The disease appears to have originated near the Port of Miami and spread north and south affecting multiple species of corals and indicating

an infectious contagion (Muller et al., 2020). Histologic examination of diseased and apparently healthy corals showed necrosis of endosymbionts and host cells indicating a widespread phenomenon (Landsberg et al., 2020). Endosymbionts are the common denominator of all species of corals in the Caribbean. A viral infection killing endosymbionts leading to host cell death and clinical manifestations of SCTLD is a reasonable hypothesis to explain the large number of coral species affected by the disease (Aeby et al., 2019). Perhaps endosymbionts in the Caribbean are particularly susceptible to viral infections in contrast to those of corals in the Pacific where lesions compatible with SCLTD at the microscopic level have yet to be documented (Williams et al., 2010; Work and Aeby, 2011; Work et al., 2012, 2014, 2015; Rodríguez-Villalobos et al., 2014, 2015). More information on endosymbionts species-specific susceptibility to potential virus infections would be of interest.

Other aspects of SCTLD would also support a virus infection of endosymbionts. Landsberg et al. (2020) found histologic lesions in corals that were apparently healthy, and we also saw endosymbiont pathology associated with AVLP in both apparently healthy and lesioned corals indicating that viral infection is widespread and enzootic. Treating lesion margins of corals affected with SCTLD stops progression of tissue loss but does not prevent the appearance of new multifocal lesions (Shilling et al., 2021) fitting the pattern of a systemic virus disease affecting endosymbionts throughout the colony where virus-induced pathology could arise anywhere either through reactivation of systemic lesions or reinfection. A possible analogy would be smallpox in humans with multicentric lesions on the skin (Councilman, 1905). We note that Landsberg et al. (2020) did not report AVLP on TEMs, and we suspect this was in part because greater effort and close scrutiny of numerous TEMs in this study allowed us to develop an image recognition pattern permitting identification of AVLP as a possible cause of endosymbiont pathology. A review of TEMs showed the ultrastructural changes seen here were similar to those from corals processed in Florida indicating that our findings are not an artifact of processing.

Reasons why a viral disease would appear in endosymbionts of Florida corals in 2014 and its origins are speculative but could relate to host cell movement, temperature, or sedimentation. Endosymbionts can move long distances. For instance, *Durusdinium* (LaJeunesse et al., 2018), was recently documented invading the Caribbean from the Pacific rendering infected host corals there less susceptible to bleaching but making them poorer depositors of calcium carbonate (Pettay et al., 2015). A similar mechanism could be responsible for introduction of novel pathogens. Alternatively, this putative virus has been present historically in Florida, but somehow environmental conditions have changed sufficiently to allow it to flourish. For instance, SCTLD was originally described in 2014 during unusually high temperatures and prior bleaching events (Precht et al., 2016). Climate change is expected to significantly alter the dynamics and spread of plant pathogens (Jones, 2012), so a plausible conjecture is that rising temperatures could have the same effect for pathogens of endosymbionts. A final possibility is sedimentation. A dredging operation in Miami harbor was ongoing during the time when SCTLD appeared in Florida that resulted in a sediment plume covering an area exceeding 200 km^2 (Barnes et al., 2015) leading to sediment deposition on corals (Miller et al., 2016). Sediments are known reservoirs of other viruses infecting marine dinoflagellates (Nagasaki et al., 2006), so perhaps dredging released viruses previously locked in deep sediments.

Endosymbiont pathology associated with AVLP was seen in both apparently healthy and SCTLD affected tissues, including from colonies from presumably SCTLD free areas. The lack of a clear pattern between presence of endosymbiont pathology, AVLP, and health status has several potential explanations. First, it is almost certain that corals were sampled in various stages of disease as no scoring was assigned to severity of gross lesions, and it was impossible to know in the field at what temporal stage of infection a coral might be. Second, there is clear evidence of differential host responses to SCTLD as manifested by differential susceptibility; for instance, the disease severely affects *D. cylindrus* (Neely et al., 2021) but hardly affects *Acropora* sp. (Alvarez-Filip et al., 2019). This difference in host response is further seen at the cellular level where histologic manifestation of disease varied inconsistently between species both in apparently healthy and lesioned tissues (Landsberg et al., 2020). Third, even within apparently normal tissues from SCTLD-enzootic areas, there was evidence of cellular pathology at the light microscopic level. Based on presence of microscopic lesions in a single *M. cavernosa* from the Florida Keys, Landsberg et al. (2020) suspected that SCTLD would have been present in the area months earlier than documented in the field grossly. We acknowledge that a majority of samples from SCTLD-free areas examined by histology had no histologic lesions (Landsberg et al., 2020), yet all samples from SCTLD-free areas examined by TEM were AVLP positive. Because TEM allows visualization of structures not visible on light microscopy, it is possible that corals from SCTLD-free areas were in early stages of viral replication but not at advanced stages sufficient to show lytic necrosis visible on light microscopy. Because cellular pathology precedes manifestation of gross lesions (Cheville, 1976), morphologic changes at the microscopic level are detected earlier than gross pathology, so it is not surprising that light microscopy could be a more sensitive tool to detect presence of disease in an ecosystem. Also, because TEM is able to detect more subtle cellular changes than light microscopy, it is possible that we simply detected early signs of disease with this tool that were not yet evident on light microscopy. Although it is possible that endosymbiont pathology has nothing to do with gross lesions of SCTLD, this would completely contravene precepts of veterinary pathology where evidence of cellular pathology is presumed to play a role in manifestation of gross pathology unless proven otherwise (Cheville, 1988). In summary, given all the variables above (differential host susceptibility, temporal variation in disease manifestation, a sampling design not structured to account for severity of disease) presence of pathology in apparently normal tissues is expected, and the potential role of viruses as a cause of SCTLD merits further investigation.

The lack of a clear pattern between gross and microscopic pathology could be rectified in future studies. If SCTLD is confirmed to be a viral disease, careful manipulative experiments using well-characterized hosts confirmed microscopically and molecularly to be virus free and tracing of gross and microscopic pathology as disease progresses temporally would go a long ways to increase our understanding of disease pathogenesis and relating microscopic to gross pathology. Given the variation in species' response to SCTLD (Alvarez-Filip et al., 2019), there is a need to develop host-specific case definitions for SCTLD which would also increase our understanding of how to relate gross to microscopic pathology. Field sampling for SCTLD might consider developing some sort of subjective disease severity score based on systematic gross descriptions (Work and Aeby, 2006). This approach has proven to be useful in other wildlife diseases. For example, for the tumor disease in green turtle (*Chelonia mydas*) fibropapillomatosis, a subjective four-point field tumor scoring system correlates well with cellular manifestation of blood pathology (Work and Balazs, 1999), host immune response (Work et al., 2001), and susceptibility to opportunistic bacterial infections (Work et al., 2003). Perhaps a similar scheme applied to corals would aid in yielding better associations between cellular and gross pathology. Our findings are a cautionary tale about depending only on gross appearance of animals to assess health or determine whether a pathogen exists in an ecosystem. Finally, the fact that AVLP associated with cell pathology were seen in apparently normal corals from areas apparently free of SCTLD, at least as manifested grossly, emphasizes the need for proper "negative controls" preferably defined based on gross and microscopic morphology.

Logical next steps would be to confirm the presence of viral infections in endosymbionts through other means. Attempts to grow and propagate the virus in culture guided by light and electron microscopy would confirm whether lesions seen in the laboratory can replicate those seen here. It would also allow for a better understanding of viral morphogenesis and host response, thus confirming or refuting our interpretation of putative developmental stages. Fortunately, endosymbionts (Taguchi and Kinzie, 2001) are more readily cultured than coral host cells (Helman et al., 2008), so this is a plausible objective. Identifying the virus through molecular means is also critical. Single-stranded RNA viruses have been identified in corals in the Caribbean through molecular means, however, none of the viruses identified to date match the morphology of AVLP seen here (Correa et al., 2013). Molecular biology of plant and algal viruses is a well-developed field (Roossinck et al., 2015), so deep sequencing to identify this putative virus is also a plausible objective. Detection of possible lytic activity by the putative AVLP seen here, and their potential mechanistic role in the mortality of endosymbionts and the associated sequential pathology of SCTLD are important next steps for investigation. It will be critical to localize the virus to the anatomic lesion through tools like *in situ* hybridization or immunohistochemistry (Mochizuki and Ohki, 2015), and fortunately, archived tissues exist to do this (Landsberg et al., 2020). Assessing whether SCTLD can be reproduced in corals known to be AVLP-negative would be important and would ease the development and validation of rapid diagnostic assays to detect the virus in the field. This would then permit a better understanding of the epidemiology of infections, possibly setting the stage for management options and interventions.

DATA AVAILABILITY STATEMENT

The raw data supporting the conclusions of this article will be made available by the authors, without undue reservation.

AUTHOR CONTRIBUTIONS

JL and ThW secured funding. YK shipped 2018 samples to ThW. ThW and TiW prepared 2018 samples for TEM, obtained and evaluated TEM images. JL and YK reviewed 2016 TEM samples. ThW, JL, YK, SC, and EP evaluated histological slides and TEM images and interpreted histopathology. ThW drafted the manuscript. All authors contributed to writing the manuscript.

FUNDING

This research was supported by United States Fish and Wildlife Service Funds for State Wildlife Grant Award FL-T-F18AF00492 awarded to FWC for sample processing for histology and TEM, and for histopathological examinations of the samples at FWRI. The Florida Coastal Office, Florida Department of Environmental Protection Coral Reef Conservation Program (order numbers BOA35A and B25636) provided supplemental funding to FWC for the field coral sample collections. The TEM samples were provided to the NWHC-Honolulu Field Station, which supported University of Hawai'i at Mānoa for TEM processing and imaging. Collections were authorized under FWC special activity license SAL-17-1702-SRP and Florida Keys National Marine Sanctuary permits: FKNMS-2016-078, FKNMS-2017-100, FKNMS-2018-006, and FKNMS-2015-156.

ACKNOWLEDGMENTS

We thank the FWC-FWRI core field sample collections staff: Nathan Berkebile, Michael Bollinger, Vanessa Brinkhuis, Katy Cummings, Ananda Ellis, Kristine Fisher, John Hart, Lindsay Huebner, Kerry Maxwell, Brian Reckenbeil, and Jennifer Stein. Paul Barbera, Tiffany Boisvert, Stephanie Schopmeyer, and William Sharp (FWC-FWRI), Sierra Hobbs (University of West Florida), Elizabeth McDonald and Karen Neely (Nova Southeastern University), Kristi Kerrigan (Florida Department of Environmental Protection), and Jason Spadaro (College of the Florida Keys) also provided assistance or operational support for the collection of coral samples. We thank FWC-FWRI staff Clark Gray for TEM assistance. Michelle Dennis provided constructive critiques of earlier versions of this manuscript. Any use of trade, firm, or product names is for descriptive purposes only and does not imply endorsement by the United States Government.

Data collected and photographs taken for this study are available at https://doi.org/10.5066/P9B6M72R, (Work et al., 2021).

SUPPLEMENTARY MATERIAL

The Supplementary Material for this article can be found online at: https://www.frontiersin.org/articles/10.3389/fmars.2021.750658/full#supplementary-material

Supplementary Figure 1 | Ultrastructure of endosymbionts and putative viral-like particles (VLP) associated with chloroplast pathology in *M. cavernosa* sampled in 2016; **(A)** Endosymbiont with multifocal vesicle formations in the chloroplast; bar = 0.5 μm. **(B)** Inset of **(A)**, higher magnification view of vesicles (arrowhead) in chloroplast **(C)**; bar = 200 nm **(C)** Vesicle in chloroplast with clumped AVLP (arrowhead); bar = 100 nm. **(D)** Higher magnification view of clumped AVLP in a chloroplast vesicle; bar = 50 nm. **(E)** Degraded endosymbiont with peripheral chloroplast, and enlarged vacuolar cavities with electron-dense inclusions and VLP; bar = 1 μm. **(F)** Inset of **(E)**, higher magnification view of vacuole with filamentous VLP (arrowheads) adjacent to the degrading chloroplast **(C)** with a vesicle (V); bar = 100 nm.

Supplementary Figure 2 | Pairwise scatterplots of percent of pathological features (lower right) and correlation coefficients (upper left) for pairwise plots. The higher the correlation, the larger the number. For the features, ED stands for electron dense bodies, TM, Indistinct stands for indistinct thylakoid membrane, and AVLP stands for anisometric viral-like particle.

REFERENCES

Ackermann, H.-W., and Tiekotter, K. L. (2012). Murphy's law-if anything can go wrong, it will: problems in phage electron microscopy. *Bacteriophage* 2, 122–129. doi: 10.4161/bact.20693

Aeby, G. S., Ushijima, B., Campbell, J. E., Jones, S., Williams, G. J., Meyer, J. L., et al. (2019). Pathogenesis of a tissue loss disease affecting multiple species of corals along the Florida reef tract. *Front. Mar. Sci.* 6:678. doi: 10.3389/fmars.2019.00678

Agrios, G. N. (2004). *Plant Pathology*. Netherlands: Elsevier.

Ahlquist, P. (2006). Parallels among positive-strand RNA viruses, reverse-transcribing viruses and double-stranded RNA viruses. *Nat. Rev. Microbiol.* 4, 371–382. doi: 10.1038/nrmicro1389

Alvarez-Filip, L., Estrada-Saldívar, N., Pérez-Cervantes, E., Molina-Hernández, A., and González-Barrios, F. J. (2019). A rapid spread of the stony coral tissue loss disease outbreak in the Mexican Caribbean. *PeerJ* 7:e8069. doi: 10.7717/peerj.8069

Barnes, B. B., Hu, C., Kovach, C., and Silverstein, R. N. (2015). Sediment plumes induced by the Port of Miami dredging: analysis and interpretation using Landsat and MODIS data. *Remote Sens. Environ.* 170, 328–339. doi: 10.1016/j.rse.2015.09.023

Bettarel, Y., Thuy, N. T., Huy, T. Q., Hoang, P. K., and Bouvier, T. (2013). Observation of virus-like particles in thin sections of the bleaching scleractinian coral *Acropora cytherea*. *J. Mar. Biol. Assoc. U. K.* 93, 909–912. doi: 10.1017/S0025315411002062

Bhattacharyya, D., and Chakraborty, S. (2018). Chloroplast: the Trojan horse in plant-virus interaction. *Mol. Plant Pathol.* 19, 504–518. doi: 10.1111/mpp.12533

Brown, B. E., and Bythell, J. C. (2005). Perspectives on mucus secretion in reef corals. *Mar. Ecol. Prog. Ser.* 296, 291–309. doi: 10.3354/MEPS296291

Camaya, A. P., Sekida, S., and Okuda, K. (2016). Changes in the ultrastructures of the coral *Pocillopora damicornis* after exposure to high temperature, ultraviolet and far-red radiation. *Cytologia* 81, 465–470. doi: 10.1508/cytologia.81.465

Cheville, N. F. (1976). *Cell Pathology*. Ames: Iowa State University Press.

Cheville, N. F. (1988). *Introduction to Veterinary Pathology*. Ames: Iowa State University Press.

Correa, A. M. S., Ainsworth, T. D., Rosales, S. M., Thurber, A. R., Butler, C. R., and Vega Thurber, R. L. (2016). Viral outbreak in corals associated with an in situ bleaching event: atypical herpes-like viruses and a new megavirus infecting *Symbiodinium*. *Front. Microbiol.* 7:127. doi: 10.3389/fmicb.2016.00127

Correa, A. M. S., Welsh, R. M., and Thurber, R. L. V. (2013). Unique nucleocytoplasmic dsDNA and +ssRNA viruses are associated with the dinoflagellate endosymbionts of corals. *ISME J.* 7, 13–27. doi: 10.1038/ismej.2012.75

Councilman, W. T. (1905). Some general considerations on the pathology of Smallpox. *Public Health Pap.* 31, 218–229.

Davy, J. E., and Patten, N. L. (2007). Morphological diversity of virus-like particles within the surface microlayer of scleractinian corals. *Aquat. Microb. Ecol.* 47, 37–44. doi: 10.3354/ame047037:

Davy, S. K., Burchett, S. G., Dale, A. L., Davies, P., Davy, J. E., Muncke, C., et al. (2006). Viruses: agents of coral disease?. *Dis. Aquat. Org.* 69, 101–110. doi: 10.3354/dao069101

Drake, J. L., Mass, T., Stolarski, J., Von Euw, S., Van De Schootbrugge, B., and Falkowski, P. G. (2020). How corals made rocks through the ages. *Glob. Change Biol.* 26, 31–53. doi: 10.1111/gcb.14912

Eaton, K. R., Landsberg, J. H., Kiryu, Y., Peters, E. C., and Muller, E. M. (2021). Measuring stony coral tissue loss disease induction and lesion progression within two intermediately susceptible species, *Montastraea cavernosa* and *Orbicella faveolata*. *Front. Mar. Sci.* 8:717265. doi: 10.3389/fmars.2021.717265

Fautin, D. G., and Mariscal, R. N. (1991). "Cnidaria: Anthozoa," in *Microscopic Anatomy of Invertebrates. Vol. 2: Placozoa, Porifera, Cnidaria, and Ctenophora*, eds F. W. Harrison and E. E. Ruppert (New York: Wiley-Liss), 267–358.

Florida Coral Disease Response Research, and Epidemiology Team (2018). *Case Definition: Stony Coral Tissue Loss Disease*. Available online at: https://floridadep.gov/sites/default/files/Copy%20of%20StonyCoralTissueLossDisease_CaseDefinition%20final%2010022018.pdf (Accessed September 27, 2021).

Grupstra, C. G. B., Howe-Kerr, L. I., Veglia, A. J., Bryant, R. L., Coy, S. R., Blackwelder, P. L., et al. (2021). Thermal stress triggers productive viral infection of a key coral reef symbiont. *BioRxiv* [Preprint]. doi: 10.1101/2021.03.17.435810

Helman, Y., Natale, F., Sherrell, R., Lavigne, M., Starovoytov, V., Gorbunov, M., et al. (2008). Extracellular matrix production and calcium carbonate precipitation by coral cells *in vitro*. *Proc. Natl. Acad. Sci. U. S. A.* 105, 54–58. doi: 10.1073/pnas.0710604105

Hyman, L. H. (1940). *The Invertebrates: Protozoa Through Ctenophora*. New York: McGraw-Hill.

Jackson, V. L. N., Allen, M. J., and Monier, A. (2021). "Viruses of eukaryotic microalgae," in *Studies in Viral Ecology*, ed. C. J. Hurst (New York: John Wiley & Sons), 89–119.

Jiang, P.-L., Pasaribu, B., and Chen, C.-S. (2014). Nitrogen-deprivation elevates lipid levels in *Symbiodinium* spp. by lipid droplet accumulation: morphological and compositional analyses. *PLoS One* 9:e87416. doi: 10.1371/journal.pone.0087416

Jin, X., Jiang, Z., Zhang, K., Wang, P., Cao, X., Yue, N., et al. (2018). Three-dimensional analysis of chloroplast structures associated with virus infection. *Plant Physiol.* 176, 282–294. doi: 10.1104/pp.17.00871

Jones, R. (2012). Influence of climate change on plant disease infections and epidemics caused by viruses and bacteria. *CAB Rev.* 7, 1–32. doi: 10.1079/PAVSNNR20127022

Kroemer, G., Galluzzi, L., Vandenabeele, P., Abrams, J., Alnemri, E. S., Baehrecke, E. H., et al. (2009). Classification of cell death: recommendations of the Nomenclature Committee on Cell Death 2009. *Cell Death Differ.* 16, 3–11. doi: 10.1038/cdd.2008.150

Ladrière, O., Compère, P., Nicole, D., Vandewalle, P., and Poulicek, M. (2008). Morphological alterations of zooxanthellae in bleached cnidarian hosts. *Cah. Biol. Mar.* 49, 215–227.

LaJeunesse, T., Parkinson, J., Gabrielson, P., Jeong, H. J., Reimer, J., Voolstra, C., et al. (2018). Systematic revision of Symbiodiniaceae highlights the antiquity and diversity of coral endosymbionts. *Curr. Biol.* 28, 2570–2580. doi: 10.1016/j.cub.2018.07.008

Landsberg, J. H. (2002). The effects of harmful algal blooms on aquatic organisms. *Rev. Fish. Sci.* 10, 113–390. doi: 10.1080/20026491051695

Landsberg, J. H., Kiryu, Y., Peters, E. C., Wilson, P. W., Perry, N., Waters, Y., et al. (2020). Stony coral tissue loss disease in Florida is associated with disruption of host–zooxanthellae physiology. *Front. Mar. Sci.* 7:576013. doi: 10.3389/fmars.2020.576013

Lawrence, S. A., Davy, J. E., Aeby, G. S., Wilson, W. H., and Davy, S. K. (2014). Quantification of virus-like particles suggests viral infection in corals affected by *Porites* tissue loss. *Coral Reefs* 33, 687–691. doi: 10.1007/s00338-014-1168-8

Levin, R. A., Voolstra, C. R., Weynberg, K. D., and Van Oppen, M. J. H. (2017). Evidence for a role of viruses in the thermal sensitivity of coral photosymbionts. *ISME J.* 11, 808–812. doi: 10.1038/ismej.2016.154

Lohr, J., Munn, C., and Wilson, W. (2007). Characterization of a latent virus-like infection of symbiotic zooxanthellae. *Appl. Environ. Microbiol.* 73, 2976–2981. doi: 10.1128/AEM.02449-06

Martelli, G. P., Adams, M. J., Kreuze, J. F., and Dolja, V. V. (2007). Family Flexiviridae: a case study in virion and genome plasticity. *Annu. Rev. Phytopathol.* 45, 73–100. doi: 10.1146/annurev.phyto.45.062806.094401

McConnaughey, T. A. (2012). Zooxanthellae that open calcium channels: implications for reef corals. *Mar. Ecol. Prog. Ser.* 460, 277–287. doi: 10.3354/meps09776

McDowell, E., and Trump, B. (1976). Histological fixatives for diagnostic light and electron microscopy. *Arch. Pathol. Lab. Med.* 100, 405–414.

McWhorter, F. P. (1965). Plant virus inclusions. *Annu. Rev. Phytopathol.* 3, 287–312. doi: 10.1146/annurev.py.03.090165.001443

Meiling, S. S., Muller, E. M., Lasseigne, D., Rossin, A., Veglia, A. J., Macknight, N., et al. (2021). Variable species responses to experimental stony coral tissue loss disease (SCTLD) exposure. *Front. Mar. Sci.* 8:670829. doi: 10.3389/fmars.2021.670829

Meyer, J. L., Castellanos-Gell, J., Aeby, G. S., Häse, C. C., Ushijima, B., and Paul, V. J. (2019). Microbial community shifts associated with the ongoing stony coral tissue loss disease outbreak on the Florida reef tract. *Front. Microbiol.* 10:2244. doi: 10.3389/fmicb.2019.02244

Miller, M. W., Karazsia, J., Groves, C. E., Griffin, S., Moore, T., Wilber, P., et al. (2016). Detecting sedimentation impacts to coral reefs resulting from dredging the Port of Miami, Florida USA. *PeerJ* 4:e2711. doi: 10.7717/peerj.2711

Mochizuki, T., and Ohki, S. T. (2015). "Detection of plant virus in meristem by immunohistochemistry and in situ hybridization," in *Plant Virology Protocols. Methods in Molecular Biology (Methods and Protocols)*, eds I. Uyeda and C. Masuta (New York: Humana Press), 275–287.

Montalvo-Proaño, J., Buerger, P., Weynberg, K. D., and Van Oppen, M. J. H. (2017). A PCR-based assay targeting the major capsid protein gene of a Dinorna-like ssRNA virus that infects coral photosymbionts. *Front. Microbiol.* 8:1665. doi: 10.3389/fmicb.2017.01665

Muller, E. M., Sartor, C., Alcaraz, N. I., and Van Woesik, R. (2020). Spatial epidemiology of the stony-coral-tissue-loss disease in Florida. *Front. Mar. Sci.* 7:163. doi: 10.3389/fmars.2020.00163

Muller-Parker, G., Lee, K. W., and Cook, C. B. (1996). Changes in the ultrastructure of symbiotic zooxanthellae (*Symbiodinium* sp., Dinophyceae) in fed and starved sea anemones maintained under high and low light. *J. Phycol.* 32, 987–994. doi: 10.1111/j.0022-3646.1996.00987.x

Nagasaki, K., Tomaru, Y., Shirai, Y., Takao, Y., and Mizumoto, H. (2006). Dinoflagellate-infecting viruses. *J. Mar. Biol. Assoc. U. K.* 86, 469–474. doi: 10.1017/S0025315406013361

Nakamura, H., Asari, T., Ohizumi, Y., Kobayashi, J. I., Yamasu, T., and Murai, A. (1993). Isolation of zooxanthellatoxins, novel vasoconstrictive substances from the zooxanthella *Symbiodinium* sp. *Toxicon* 31, 371–376. doi: 10.1016/0041-0101(93)90172-F

Neely, K. L., Lewis, C. L., Lunz, K. S., and Kabay, L. (2021). Rapid population decline of the pillar coral *Dendrogyra cylindrus* along the Florida reef tract. *Front. Mar. Sci.* 8:656515. doi: 10.3389/fmars.2021.656515

Neely, K. L., Macaulay, K. A., Hower, E. K., and Dobler, M. A. (2020). Effectiveness of topical antibiotics in treating corals affected by Stony Coral Tissue Loss Disease. *PeerJ* 8:e9289. doi: 10.7717/peerj.9289

Netherton, C., Moffat, K., Brooks, E., and Wileman, T. (2007). A guide to viral inclusions, membrane rearrangements, factories, and viroplasm produced during virus replication. *Adv. Virus Res.* 70, 101–182. doi: 10.1016/s0065-3527(07)70004-0

Patten, N. L., Harrison, P. L., and Mitchell, J. G. (2008). Prevalence of virus-like particles within a staghorn scleractinian coral (*Acropora muricata*) from the Great Barrier Reef. *Coral Reefs* 27, 569–580. doi: 10.1007/s00338-008-0356-9

Pettay, D. T., Wham, D. C., Smith, R. T., Iglesias-Prieto, R., and Lajeunesse, T. C. (2015). Microbial invasion of the Caribbean by an Indo-Pacific coral zooxanthella. *Proc. Natl. Acad. Sci. U. S. A.* 112, 7513. doi: 10.1073/pnas.1502283112

Piggot, A. M., Fouke, B. W., Sivaguru, M., Sanford, R. A., and Gaskins, H. R. (2009). Change in zooxanthellae and mucocyte tissue density as an adaptive response to environmental stress by the coral, *Montastraea annularis*. *Mar. Biol.* 156, 2379–2389. doi: 10.1007/s00227-009-1267-1

Precht, W. F., Gintert, B. E., Robbart, M. L., Fura, R., and Van Woesik, R. (2016). Unprecedented disease-related coral mortality in southeastern Florida. *Sci. Rep.* 6:31374. doi: 10.1038/srep31374

R Core Team (2017). *R: A Language and Environment for Statistical Computing*. Vienna: R Foundation for Statistical Computing.

Reft, A. J. (2012). *Understanding the Morphology and Distribution of Nematocysts in Sea Anemones and their Relatives*. Ph.D. thesis. Columbus: The Ohio State University.

Reynolds, E. S. (1963). The use of lead citrate at high pH as an electron-opaque stain in electron microscopy. *J. Cell Biol.* 17, 208–212. doi: 10.1083/jcb.17.1.208

Rodríguez-Villalobos, J. C., Rocha-Olivares, A., Work, T. M., Calderon-Aguilera, L. E., and Cáceres-Martínez, J. A. (2014). Gross and microscopic pathology of lesions in *Pocillopora* spp. from the subtropical eastern Pacific. *J. Invertebr. Pathol.* 120, 9–17. doi: 10.1016/j.jip.2014.04.007

Rodríguez-Villalobos, J. C., Work, T. M., Calderon-Aguilera, L. E., Reyes-Bonilla, H., and Hernández, L. (2015). Explained and unexplained tissue loss in corals from the Tropical Eastern Pacific. *Dis. Aquat. Org.* 116, 121–131. doi: 10.3354/dao02914

Roossinck, M. J., Martin, D. P., and Roumagnac, P. (2015). Plant virus metagenomics: advances in virus discovery. *Phytopathology* 105, 716–727. doi: 10.1094/PHYTO-12-14-0356-RVW

Rosales, S. M., Clark, A. S., Huebner, L. K., Ruzicka, R. R., and Muller, E. M. (2020). Rhodobacterales and Rhizobiales are associated with stony coral tissue loss disease and its suspected sources of transmission. *Front. Microbiol.* 11:681. doi: 10.3389/fmicb.2020.00681

Rosset, S., D'angelo, C., and Wiedenmann, J. (2015). Ultrastructural biomarkers in symbiotic algae reflect the availability of dissolved inorganic nutrients and particulate food to the reef coral holobiont. *Front. Mar. Sci.* 2:103. doi: 10.3389/fmars.2015.00103

Shilling, E. N., Combs, I. R., and Voss, J. D. (2021). Assessing the effectiveness of two intervention methods for stony coral tissue loss disease on *Montastraea cavernosa*. *Sci. Rep.* 11:8566. doi: 10.1038/s41598-021-86926-4

Sowden, R. G., Watson, S. J., and Jarvis, P. (2017). The role of chloroplasts in plant pathology. *Essays Biochem.* 62, 21–39. doi: 10.1042/ebc20170020

Starborg, T., Kalson, N. S., Lu, Y., Mironov, A., Cootes, T. F., Holmes, D. F., et al. (2013). Using transmission electron microscopy and 3View to determine collagen fibril size and three-dimensional organization. *Nat. Protoc.* 8, 1433–1448. doi: 10.1038/nprot.2013.086

Stevens, W. A. (1983). "Plant Virus Structure," in *Virology of Flowering Plants*. (Boston: Springer), 69–93. Available online at: https://link.springer.com/book/10.1007/978-1-4757-1251-3

Taguchi, S., and Kinzie, R. A. (2001). Growth of zooxanthellae in culture with two nitrogen sources. *Mar. Biol.* 138, 149–155. doi: 10.1007/s002270000435

Taylor, D. L. (1968). In situ studies on the cytochemistry and ultrastructure of a symbiotic marine dinoflagellate. *J. Mar. Biol. Assoc. U. K.* 48, 349–366. doi: 10.1017/S0025315400034548

Tomaru, Y., Hata, N., Masuda, T., Tsuji, M., Igata, K., Masuda, Y., et al. (2007). Ecological dynamics of the bivalve-killing dinoflagellate *Heterocapsa circularisquama* and its infectious viruses in different locations of western Japan. *Environ. Microbiol.* 9, 1376–1383. doi: 10.1111/j.1462-2920.2007.01252.x

Tomaru, Y., and Nagasaki, K. (2004). Widespread occurrence of viruses lytic to the bivalve-killing dinoflagellate *Heterocapsa circularisquama* along the western coast of Japan. *Plankton Biol. Ecol.* 51, 1–6.

Trench, R. K., and Blank, R. J. (1987). *Symbiodinium microadriaticum* Freudenthal, *S. goreauii* sp. nov., *S. kawagutii* sp. nov. and *S. pilosum* sp. nov.: gymnodinioid

dinoflagellate symbionts of marine invertebrates. *J. Phycol.* 23, 469–481. doi: 10.1111/j.1529-8817.1987.tb02534.x

Ushijima, B., Meyer, J. L., Thompson, S., Pitts, K., Marusich, M. F., Tittl, J., et al. (2020). Disease diagnostics and potential coinfections by *Vibrio coralliilyticus* during an ongoing coral disease outbreak in Florida. *Front. Microbiol.* 11:569354. doi: 10.3389/fmicb.2020.569354

van Doorn, W. G., Beers, E. P., Dangl, J. L., Franklin-Tong, V. E., Gallois, P., Hara-Nishimura, I., et al. (2011). Morphological classification of plant cell deaths. *Cell Death Differ.* 18, 1241–1246. doi: 10.1038/cdd.2011.36

van Oppen, M. J. H., Leong, J., and Gates, R. D. (2009). Coral-virus interactions: a double-edged sword?. *Symbiosis* 47, 1–8. doi: 10.1007/BF03179964

Vega Thurber, R. L., and Correa, A. M. S. (2011). Viruses of reef-building scleractinian corals. *J. Exp. Mar. Biol. Ecol.* 408, 102–113. doi: 10.1016/j.jembe.2011.07.030

Vega-Thurber, R., Payet, J. P., Thurber, A. R., and Correa, A. M. S. (2017). Virus–host interactions and their roles in coral reef health and disease. *Nat. Rev. Microbiol.* 15, 205–216. doi: 10.1038/nrmicro.2016.176

Wakefield, T. S., Farmer, M. A., and Kempf, S. C. (2000). Revised description of the fine structure of in situ zooxanthellae genus *Symbiodinium*. *Biol. Bull.* 19, 76–84. doi: 10.2307/1542709

Walker, B. K., Turner, N. R., Noren, H. K. G., Buckley, S. F., and Pitts, K. A. (2021). Optimizing stony coral tissue loss disease (SCTLD) intervention treatments on *Montastraea cavernosa* in an endemic zone. *Front. Mar. Sci.* 8:666224. doi: 10.3389/fmars.2021.666224

Weng, L.-C., Pasaribu, B., Ping Lin, I., Tsai, C.-H., Chen, C.-S., and Jiang, P.-L. (2014). Nitrogen deprivation induces lipid droplet accumulation and alters fatty acid metabolism in symbiotic dinoflagellates isolated from *Aiptasia pulchella*. *Sci. Rep.* 4:5777. doi: 10.1038/srep05777

Weynberg, K. D., Neave, M., Clode, P. L., Voolstra, C. R., Brownlee, C., Laffy, P., et al. (2017). Prevalent and persistent viral infection in cultures of the coral algal endosymbiont *Symbiodinium*. *Coral Reefs* 36, 773–784. doi: 10.1007/s00338-017-1568-7

Williams, G. J., Work, T. M., Aeby, G. S., Knapp, I. S., and Davy, S. K. (2010). Gross and microscopic morphology of lesions in Cnidaria from Palmyra Atoll, Central Pacific. *J. Invertebr. Pathol.* 106, 165–170. doi: 10.1016/j.jip.2010.08.002

Wilson, W. H., Dale, A. L., Davy, J. E., and Davy, S. K. (2005). An enemy within? Observations of virus-like particles in reef corals. *Coral Reefs* 24, 145–148. doi: 10.1007/s00338-004-0448-0

Wilson, W. H., Francis, I., Ryan, K., and Davy, S. K. (2001). Temperature induction of viruses in symbiotic dinoflagellates. *Aquat. Microb. Ecol.* 25, 99–102. doi: 10.3354/ame025099

Wood-Charlson, E. M., Weynberg, K. D., Suttle, C. A., Roux, S., and Van Oppen, M. J. (2015). Metagenomic characterization of viral communities in corals: mining biological signal from methodological noise. *Environ. Microbiol.* 17, 3440–3449. doi: 10.1111/1462-2920.12803

Work, T., and Meteyer, C. (2014). To understand coral disease, look at coral cells. *Ecohealth* 11, 610–618. doi: 10.1007/s10393-014-0931-1

Work, T. M., and Aeby, G. S. (2006). Systematically describing gross lesions in corals. *Dis. Aquat. Org.* 70, 155–160. doi: 10.3354/dao070155

Work, T. M., and Aeby, G. S. (2011). Pathology of tissue loss (white syndrome) in *Acropora* sp. corals from the Central Pacific. *J. Invertebr. Pathol.* 107, 127–131. doi: 10.1016/j.jip.2011.03.009

Work, T. M., Aeby, G. S., and Hughen, K. (2015). Gross and microscopic pathology of corals from Micronesia. *Vet. Pathol.* 53, 153–162. doi: 10.1177/0300985815571669

Work, T. M., Aeby, G. S., Lasne, G., and Tribollet, A. (2014). Gross and microscopic pathology of hard and soft corals in New Caledonia. *J. Invertebr. Pathol.* 120, 50–58. doi: 10.1016/j.jip.2014.05.007

Work, T. M., and Balazs, G. H. (1999). Relating tumor score to hematology in green turtles with fibropapillomatosis in Hawaii. *J. Wildl. Dis.* 35, 804–807. doi: 10.7589/0090-3558-35.4.804

Work, T. M., Balazs, G. H., Wolcott, M., and Morris, R. M. (2003). Bacteraemia in Hawaiian green turtles, *Chelonia mydas*, with fibropapillomatosis. *Dis. Aquat. Org.* 53, 41–46. doi: 10.3354/dao053041

Work, T. M., Dagenais, J., Weatherby, T. M., Balazs, G. H., and Ackermann, M. (2017). *In vitro* replication of Chelonid Herpesvirus 5 in organotypic skin cultures from Hawaiian green turtles (*Chelonia mydas*). *J. Virol.* 91, e00404–e00417. doi: 10.1128/jvi.00404-17

Work, T. M., Rameyer, R. A., Balazs, G. H., Cray, C., and Chang, S. P. (2001). Immune status of free-ranging green turtles with fibropapillomatosis from Hawaii. *J. Wildl. Dis.* 37, 574–581. doi: 10.7589/0090-3558-37.3.574

Work, T. M., Russell, R., and Aeby, G. S. (2012). Tissue loss (white syndrome) in the coral *Montipora capitata* is a dynamic disease with multiple host responses and potential causes. *Proc. R. Soc. Lond. B Biol. Sci.* 279, 4334–4341. doi: 10.1098/rspb.2012.1827

Work, T. M., Weatherby, T. M., Landsberg, J. H., Kiryu, Y., Cook, S. M., and Peters, E. C. (2021). *Viral-like particles are associated with endosymbiont pathology in Florida corals affected by stony coral tissue loss disease. U.S. Geological Survey data release*. Reston, VA: U. S. Geological Survey.

Yang, X., Zhang, T., Chen, B., and Zhou, G. (2017). Transmission biology of rice stripe mosaic virus by an efficient insect vector *Recilia dorsalis* (Hemiptera: Cicadellidae). *Front. Microbiol.* 8:2457. doi: 10.3389/fmicb.2017.02457

Yellowlees, D., Rees, T., Alwyn, V., and Leggat, W. (2008). Metabolic interactions between algal symbionts and invertebrate hosts. *Plant Cell Environ.* 31, 679–694. doi: 10.1111/j.1365-3040.2008.01802.x

Zechmann, B., and Zellnig, G. (2009). Rapid diagnosis of plant virus diseases by transmission electron microscopy. *J. Virol. Methods* 162, 163–169. doi: 10.1016/j.jviromet.2009.07.032

Zhao, J., Zhang, X., Hong, Y., and Liu, Y. (2016). Chloroplast in plant-virus interaction. *Front. Microbiol.* 7:1565. doi: 10.3389/fmicb.2016.01565

Zhu, B., Pan, K., and Wang, G. (2011). Effects of host starvation on the symbiotic dinoflagellates from the sea anemone *Stichodactyla mertensii*. *Mar. Ecol.* 32, 15–23. doi: 10.1111/j.1439-0485.2010.00405.x

Conflict of Interest: The authors declare that the research was conducted in the absence of any commercial or financial relationships that could be construed as a potential conflict of interest.

Publisher's Note: All claims expressed in this article are solely those of the authors and do not necessarily represent those of their affiliated organizations, or those of the publisher, the editors and the reviewers. Any product that may be evaluated in this article, or claim that may be made by its manufacturer, is not guaranteed or endorsed by the publisher.